

Research Article

Closed-Form Distance Estimators under Kalman Filtering Framework with Application to Object Tracking

Vladimir Shin ¹, Georgy Shevlyakov,² Woohyun Jeong,³ and Yoonsoo Kim ³

¹Department of Information and Statistics, Research Institute of Natural Science, Gyeongsang National University, Jinju 52828, Republic of Korea

²Department of Applied Mathematics, Peter the Great St. Petersburg Polytechnic University, Saint Petersburg 195251, Russia

³Graduate School of Mechanical and Aerospace Engineering, Gyeongsang National University, Jinju 52828, Republic of Korea

Correspondence should be addressed to Yoonsoo Kim; yunsoo@gnu.ac.kr

Received 9 April 2020; Revised 15 June 2020; Accepted 24 June 2020; Published 20 August 2020

Academic Editor: António M. Lopes

Copyright © 2020 Vladimir Shin et al. This is an open access article distributed under the Creative Commons Attribution License, which permits unrestricted use, distribution, and reproduction in any medium, provided the original work is properly cited.

In this paper, the minimum mean square error (MMSE) estimation problem for calculation of distances between two signals via the Kalman filtering framework is considered. The developed algorithm includes two stages: the Kalman estimate of a state vector computed at the first stage is nonlinearly transformed at the second stage based on a distance function and the MMSE criterion. In general, the most challenging aspect of application of the distance estimator is calculation of the multivariate Gaussian integral. However, it can be successfully overcome for the specific metrics between two points in line, between point and line, between point and plane, and others. In these cases, the MMSE estimator is defined by an analytical closed-form expression. We derive the exact closed-form bilinear and quadratic MMSE estimators that can be effectively applied for calculation of an inner product, squared norm, and Euclidean distance. A novel low-complexity suboptimal estimator for special composite functions of linear, bilinear, and quadratic forms is proposed. Radar range-angle responses are described by the functions. The proposed estimators are validated through a series of experiments using real models and metrics. Experimental results show that the MMSE estimators outperform existing estimators that calculate distance and angle in nonoptimal manner.

1. Introduction

The problem of measuring the distance between real-valued signals or images arises in most areas of scientific research. In particular, the familiar Euclidean distance plays a prominent role in many important application contexts not only in engineering, economics, statistics, and decision theory, but also in fields such as machine learning, cryptography, image recognition, and others. The statistical methods related to the distance estimation can be categorized into image and signal processing areas.

The concept of a distance metric is widely used in image processing and computer vision [1–5] (also see references therein). The distance provides a quantitative measure of the degree of match between two images or objects. These objects might be two profiles of persons, a person and a target profile, camera of a robot and people, or any two

vectors taken across the same features (variables) derived from color, shape, and/or texture information. Image similarity measures play an important role in many image algorithms and applications including retrieval, classification, change detection, quality evaluation, and registration [6–12].

The proposed paper deals with the distance estimation between random signals. In signal processing, a good distance metric helps in improving the performance of classification, clustering and localization in wireless sensor networks, radar tracking, and other applications [13–20]. The Bayesian classification approach based on concepts of the Euclidean and Mahalanobis distances is often used in discriminant analysis. Survey of the classification procedures which minimize a distance between raw signals and classes in multifeature space is given in [21, 22]. The distance estimation algorithm based on the goodness-of-fit functions

where the best parameters of the fitting functions are calculated given the training data is considered in [23]. Algorithm for estimation of a walking distance using a wrist-mounted inertial measurement unit device is proposed in [24]. The concept of distance between two samples or between two variables is fundamental in statistics due to the fact that a sum of squares of independent normal random variables has a chi-square distribution. Knowledge of the distribution and usage of the usual approximations make a confidence interval for distance metrics [25, 26]. Usage of the Taylor series expansions for aircraft geometric-height estimation using range and bearing measurements is addressed in [27, 28]. The minimum mean square error (MMSE) estimation of a state vector in the presence of information about the absolute value of a difference between its subvectors is proposed in [29].

In many applications, it is interesting to estimate not only a position or state of an object but also a nonlinear distance function which gives information to effectively control target tracking. However, most authors have not focused on a simultaneous estimation of a state and distance functions in dynamical models such as a Kalman filtering framework.

The problem of estimation of the distance function, $d_k = d(\mathbf{x}_k, \mathbf{y}_k)$, between two vector signals \mathbf{x}_k and \mathbf{y}_k is considered in the paper, but its difference from the aforementioned references is that the both signals \mathbf{x}_k and \mathbf{y}_k are unknown, and they should be simultaneously estimated with the function d_k using indirect measurements. For example, we observe positions of two points $A(\mathbf{x}_k)$ and $B(\mathbf{y}_k)$ in a line and a distance between the points represents the absolute difference, i.e., $d_k(A, B) = |\mathbf{x}_k - \mathbf{y}_k|$. The positions \mathbf{x}_k and \mathbf{y}_k and consequently the distance $d_k = |\mathbf{x}_k - \mathbf{y}_k|$ are unknown, and our problem is to optimally calculate three estimates $\hat{\mathbf{x}}_k$, $\hat{\mathbf{y}}_k$, and \hat{d}_k . Note that the simple distance estimator $\hat{d}_k = |\hat{\mathbf{x}}_k - \hat{\mathbf{y}}_k|$ is not an optimal solution.

The purpose of the paper is to derive an analytical closed-form MMSE estimator for distance functions between random signals such as the absolute value, the Euclidean distance, inner product, bilinear, and quadratic forms. The advantage of the estimator is quick and accurate calculation of distance metrics compared to the approximate or iterative estimators. A further study of using the estimators is also done for the object tracking problem where we can obtain important practical results for the distance estimation of signals in linear Gaussian discrete-time systems.

The following list highlights the primary contributions of this paper:

- (1) Extension of the MMSE approach to the estimation of a nonlinear functions of a state vector within the Kalman filtering framework. The obtained MMSE-optimal solution represents a two-stage estimator.
- (2) Derivation of analytical expressions for the different metrics between two points in a line, between a point and a line, and between a point and a plane. We establish that the obtained estimators represent compact closed-form formulas depending on the Kalman filter state estimates and error covariance.

- (3) The MMSE estimators for quadratic and bilinear forms of a state vector are investigated and applied, including the estimators for the square of a norm $\|\mathbf{x}_k\|_2^2$, the square of the Euclidean distance $\|\mathbf{x}_k - \mathbf{y}_k\|_2^2$, and the inner product $\langle \mathbf{x}_k, \mathbf{y}_k \rangle$. A novel low-complexity algorithm for suboptimal estimation of a special class of composite functions is proposed. Tracking radar responses such as range, angles, and range rate are described by the functions.
- (4) Performance of the proposed MMSE estimators through real examples illustrates their theoretical and practical usefulness.

This paper is organized as follows. Section 2 presents a statement of the MMSE estimation problem for an arbitrary nonlinear function of a state vector within a Kalman filtering framework. In Section 3, the general MMSE estimator is proposed, and computational complexity of the estimator is discussed. The concept of a closed-form estimator is introduced. In Section 4, the closed-form MMSE estimator for absolute value of a linear form of a state vector is derived (Theorem 1). In particular cases, the estimator calculates distances between two points in 1-D line, between a point and line in 2-D plane, and between a point and plane in 3-D space. The comparative analysis of the estimator via several practical examples is presented. In Section 5, the MMSE estimators for quadratic and bilinear forms of a state vector are comprehensively studied (Theorems 2 and 3). Effective matrix formulas for the quadratic and bilinear MMSE estimators are derived and applied with the Euclidean distance, a norm, and inner product of vector signals. In Section 6, a low-complexity suboptimal estimator for composite nonlinear functions is proposed and recommended for calculation of radar range-angle responses. In Section 7, the efficiency of the suboptimal estimator is demonstrated on an 2-D dynamical model. Finally, we conclude the paper in Section 8. The list of main notations is given in Table 1.

2. Problem Statement

The basic framework for the Kalman filter involves estimation of a state of a discrete-time linear dynamical system with additive Gaussian white noise:

$$\begin{aligned} \mathbf{x}_{k+1} &= \mathbf{F}_k \mathbf{x}_k + \mathbf{G}_k \mathbf{v}_k, \quad k = 0, 1, \dots, \\ \mathbf{y}_k &= \mathbf{H}_k \mathbf{x}_k + \mathbf{w}_k, \end{aligned} \quad (1)$$

where $\mathbf{x}_k \in \mathbb{R}^n$ is a state vector, $\mathbf{y}_k \in \mathbb{R}^m$ is a measurement vector, and $\mathbf{v}_k \in \mathbb{R}^r$ and $\mathbf{w}_k \in \mathbb{R}^m$ are zero-mean Gaussian white noises with process (\mathbf{Q}_k) and measurement (\mathbf{R}_k) noise covariances, respectively, i.e., $\mathbf{v}_k \sim \mathcal{N}(0, \mathbf{Q}_k)$, $\mathbf{w}_k \sim \mathcal{N}(0, \mathbf{R}_k)$, and $\mathbf{F}_k \in \mathbb{R}^{n \times n}$, $\mathbf{G}_k \in \mathbb{R}^{n \times r}$, $\mathbf{Q}_k \in \mathbb{R}^{r \times r}$, $\mathbf{R}_k \in \mathbb{R}^{m \times m}$, and $\mathbf{H}_k \in \mathbb{R}^{m \times n}$. The initial state $\mathbf{x}_0 \sim \mathcal{N}(\mathbf{m}_0, \mathbf{C}_0)$ and the process and measurement noises \mathbf{v}_k , \mathbf{w}_k are mutually uncorrelated.

In parallel with the state-space model (1), consider the nonlinear function of a state vector:

$$z_k = f(\mathbf{x}_k): \mathbb{R}^n \longrightarrow \mathbb{R}, \quad (2)$$

which in particular case represents a distance metric in \mathbb{R}^n .

TABLE 1: List of main notations.

\mathbb{R}^n	Set of n -dimensional real column vectors
$\mathbb{R}^{n \times m}$	Set of $n \times m$ real matrices
\mathbf{A}^T	Transpose of matrix \mathbf{A}
\mathbf{I}_n	Identity matrix of size $n \times n$
\mathbf{O}_n	Null matrix of size $n \times n$
\mathbf{A}^{-1}	Inverse of $n \times n$ matrix \mathbf{A}
$\text{tr}(\mathbf{A})$	Trace of $n \times n$ matrix \mathbf{A}
$\mathbb{N}(\mathbf{m}, \mathbf{C})$	Normal distribution with mean \mathbf{m} and covariance matrix \mathbf{C}
$\mathbb{E}(\cdot)$	Expectation operator
$\text{Cov}(\mathbf{x}_k)$	Covariance (covariance matrix) of random vector \mathbf{x}_k
$\text{Cov}(\mathbf{x}_k, \mathbf{y}_k)$	Cross covariance of random vectors \mathbf{x}_k and \mathbf{y}_k
$\ \mathbf{x}\ _2$	Euclidean norm (2-norm) of vector, $\ \mathbf{x}\ _2 = \sqrt{\mathbf{x}^T \mathbf{x}}$
$\langle \mathbf{x}, \mathbf{y} \rangle$	Inner product of vectors, $\langle \mathbf{x}, \mathbf{y} \rangle = \sum_{i=1}^n x_i y_i$, $\mathbf{x}, \mathbf{y} \in \mathbb{R}^n$
$\mathbf{c}^T \mathbf{x}$	Linear form (LF), $\mathbf{c}^T \mathbf{x} = \sum_{i=1}^n c_i x_i$, $\mathbf{c}, \mathbf{x} \in \mathbb{R}^n$
$\mathbf{x}^T \mathbf{A} \mathbf{x}$	Quadratic form (QF), $\mathbf{x}^T \mathbf{A} \mathbf{x} = \sum_{i,j=1}^n a_{ij} x_i x_j$, $\mathbf{A} = [a_{ij}]$
$\mathbf{x}^T \mathbf{B} \tilde{\mathbf{x}}$	Bilinear form (BLF), $\mathbf{x}^T \mathbf{A} \tilde{\mathbf{x}} = \sum_{i,j=1}^n b_{ij} x_i \tilde{x}_j$, $\mathbf{B} = [b_{ij}]$

Given the overall noisy measurements $\mathbf{y}^k = \{\mathbf{y}_1, \mathbf{y}_2, \dots, \mathbf{y}_k\}$, $k \geq 1$, our goal is to desire optimal estimators $\hat{\mathbf{x}}_k$ and \hat{z}_k for the state vector (1) and nonlinear function (2), respectively.

There are a multitude of statistics-based methods to estimate the unknown value $z_k = f(\mathbf{x}_k)$ from the sensor measurements \mathbf{y}^k . We focus on the MMSE approach, which minimizes the mean square error (MSE), $\min_{\hat{z}} \mathbb{E}(\|z_k - \hat{z}_k\|_2^2)$, which is a common measure of estimator quality.

The MMSE estimator is the conditional mean (expectation) of the unknown $z_k = f(\mathbf{x}_k)$ given the known observed value of the measurements, $\hat{z}_k^{\text{opt}} = \mathbb{E}(z_k | \mathbf{y}^k)$ [30, 31]. The most challenging problem in the MMSE approach is how to calculate the conditional mean. In this paper, explicit formulas for distance metrics within the Kalman filtering framework are derived.

3. General Formula for Optimal Two-Stage MMSE Estimator

In this section, the optimal MMSE estimator for the general function $f(\mathbf{x}_k)$ of a state vector is proposed. It includes two stages: the optimal Kalman estimate of the state vector $\hat{\mathbf{x}}_k$ computed at the first stage is used at the second stage for estimation of $f(\mathbf{x}_k)$.

First stage (calculation of Kalman estimate): the mean square estimate $\hat{\mathbf{x}}_k = \mathbb{E}(\mathbf{x}_k | \mathbf{y}^k)$ of the state \mathbf{x}_k based on the measurements \mathbf{y}^k and error covariance $\mathbf{P}_k = \text{Cov}(\mathbf{e}_k)$, $\mathbf{e}_k = \mathbf{x}_k - \hat{\mathbf{x}}_k$ are described by the recursive Kalman filter (KF) equations [30, 31]:

$$\begin{aligned}
 \hat{\mathbf{x}}_{k+1}^- &= \mathbf{F}_k \hat{\mathbf{x}}_k, \hat{\mathbf{x}}_0 = \mathbf{m}_0, \quad k = 0, 1, \dots, \\
 \mathbf{P}_{k+1}^- &= \mathbf{F}_k \mathbf{P}_k \mathbf{F}_k^T + \mathbf{G}_k \mathbf{Q}_k \mathbf{G}_k^T, \quad \mathbf{P}_0 = \mathbf{C}_0, \\
 \mathbf{K}_{k+1} &= \mathbf{P}_{k+1}^- \mathbf{H}_{k+1}^T (\mathbf{H}_{k+1} \mathbf{P}_{k+1}^- \mathbf{H}_{k+1}^T + \mathbf{R}_{k+1})^{-1}, \quad (3) \\
 \hat{\mathbf{x}}_{k+1} &= \hat{\mathbf{x}}_{k+1}^- + \mathbf{K}_{k+1} (\mathbf{y}_{k+1} - \mathbf{H}_{k+1} \hat{\mathbf{x}}_{k+1}^-), \\
 \mathbf{P}_{k+1} &= (\mathbf{I}_n - \mathbf{K}_{k+1} \mathbf{H}_{k+1}) \mathbf{P}_{k+1}^-,
 \end{aligned}$$

where $\hat{\mathbf{x}}_{k+1}^- = \mathbb{E}(\mathbf{x}_{k+1} | \mathbf{y}^k)$ and $\mathbf{P}_{k+1}^- = \text{Cov}(\mathbf{e}_{k+1}^-)$, $\mathbf{e}_{k+1}^- = \mathbf{x}_{k+1} - \hat{\mathbf{x}}_{k+1}^-$ are the time update estimate and error covariance, respectively, and $\mathbf{K}_k \in \mathbb{R}^{n \times m}$ is the filter gain matrix.

Second stage (optimal MMSE estimator): next, the optimal MMSE estimate of the nonlinear function $z_k = f(\mathbf{x}_k)$ based on the measurements \mathbf{y}^k also represents a conditional mean, that is,

$$\hat{z}_k^{\text{opt}} = \mathbb{E}(z_k | \mathbf{y}^k) = \int_{\mathbb{R}^n} f(\mathbf{x}) p(\mathbf{x} | \mathbf{y}^k) d\mathbf{x}, \quad (4)$$

where $p(\mathbf{x} | \mathbf{y}^k) = \mathbb{N}(\hat{\mathbf{x}}_k, \mathbf{P}_k)$ is a multivariate conditional Gaussian probability density function.

$$\mathbb{N}(\hat{\mathbf{x}}_k, \mathbf{P}_k) = \frac{1}{(2\pi)^{n/2} |\mathbf{P}_k|^{1/2}} \exp\left[-\frac{1}{2} (\mathbf{x} - \hat{\mathbf{x}}_k)^T \mathbf{P}_k^{-1} (\mathbf{x} - \hat{\mathbf{x}}_k)\right]. \quad (5)$$

Thus, the best estimate in equation (4) represents the optimal MMSE estimator, $\hat{z}_k^{\text{opt}} = F(\hat{\mathbf{x}}_k, \mathbf{P}_k)$, which depends on the Kalman estimate $\hat{\mathbf{x}}_k$ and error covariance \mathbf{P}_k determined by KF equation (3).

Remark 1 (closed-form MMSE estimator). In general case, the calculation of the optimal estimate, $\hat{z}_k^{\text{opt}} = \mathbb{E}(z_k | \mathbf{y}^k)$, is reduced to calculation of the multivariate Gaussian integral (5). The lack of the estimate is impossibility to calculate the integral in explicit form for the arbitrary nonlinear function $f(\mathbf{x})$. Analytical calculation of the integral (closed-form MMSE estimator) is possible only in special cases considered in the paper. The closed-form estimators for distance metrics in terms of $\hat{\mathbf{x}}_k$ and \mathbf{P}_k are proposed in Sections 4 and 5.

The Euclidean distance between two points, $x_1, x_2 \in \mathbb{R}^n$, is defined as

$$d(x_1, x_2) \stackrel{\text{def}}{=} \|x_1 - x_2\|_2 = \sqrt{\sum_{i=1}^n (x_{1,i} - x_{2,i})^2}. \quad (6)$$

In this particular case where x_1 and x_2 represent two points located on the 1-D line, the Euclidean distance represents the absolute value (see Figure 1), i.e.,

$$d(x_1, x_2) = |x_1 - x_2|. \quad (7)$$

In Section 4, the MMSE estimator for the absolute value is comprehensively studied.

4. Closed-Form MMSE Estimator for Absolute Value

4.1. MMSE Estimator for Absolute Value of Linear Form

Lemma 1 (MMSE estimator for $|x|$). *Let $x \in \mathbb{R}$ be a normal random variable, and \hat{x} and $P = \mathbb{E}(x - \hat{x})^2$ are the MMSE estimate and error variance, respectively. Then, the MMSE estimator for the absolute value $z = |x|$ has the following closed-form expression:*

$$\hat{z}^{\text{opt}} = \mathbb{E}(|x| | \mathbf{y}^k) = \sqrt{\frac{2P}{\pi}} \exp\left(-\frac{\hat{x}^2}{2P}\right) + \hat{x} \left[1 - 2\Phi\left(-\frac{\hat{x}}{\sqrt{P}}\right)\right], \quad (8)$$

where $\Phi(\cdot)$ is the cumulative distribution function of the standard normal distribution, $\mathbb{N}(0, 1)$.

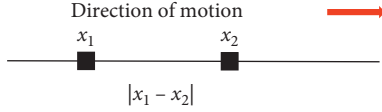


FIGURE 1: Distance $d(x_1, x_2) = |x_1 - x_2|$ between two moving points in 1-D line.

The derivation of equation (8) is given in the Appendix.

Let $\ell = \mathbf{c}^T \mathbf{x} + d$ be a linear form (LF) of the normal random vector, $\mathbf{x} \in \mathbb{R}^n$, and $\hat{\mathbf{x}} \in \mathbb{R}^n$ and $\mathbf{P} \in \mathbb{R}^{n \times n}$ are the MMSE estimate and error covariance, respectively. Then, the MMSE estimate of the linear form ℓ and its error variance can be calculated as

$$\begin{aligned} \hat{\ell} &= \mathbb{E}(\ell | \mathbf{y}^k) = \mathbf{c}^T \hat{\mathbf{x}} + d, \\ P^{(\ell)} &= \mathbb{E}(\ell - \hat{\ell})^2 = \mathbf{c}^T \mathbf{P} \mathbf{c}, \end{aligned} \quad (9)$$

and we have the following theorem.

Theorem 1 (MMSE estimator for absolute value of LF). *Let $\mathbf{x} \in \mathbb{R}^n$ be a normal random vector, and $\hat{\mathbf{x}} \in \mathbb{R}^n$ and $\mathbf{P} \in \mathbb{R}^{n \times n}$ are the MMSE estimate and error covariance, respectively. Then, the closed-form MMSE estimator for the absolute value $z = |\mathbf{c}^T \mathbf{x} + d|$ is defined by formula (8):*

$$\hat{z}^{\text{opt}} = \sqrt{\frac{2P^{(\ell)}}{\pi}} \exp\left(-\frac{\hat{\ell}^2}{2P^{(\ell)}}\right) + \hat{\ell} \left[1 - 2\Phi\left(-\frac{\hat{\ell}}{\sqrt{P^{(\ell)}}}\right)\right], \quad (10)$$

where $\hat{\ell}$ and $P^{(\ell)}$ are determined by equation (9).

The MMSE estimator (10) allows to calculate distances measured in terms of the absolute value in n -dimensional space.

4.2. Examples of MMSE Estimator for Distance between Points. Let $\mathbf{x}_k \in \mathbb{R}^n$ be a normal state vector, and $\hat{\mathbf{x}}_k \in \mathbb{R}^n$ and $\mathbf{P}_k \in \mathbb{R}^{n \times n}$ are the Kalman estimate and error covariance, respectively, $\mathbf{P}_k = [P_{ij,k}]$.

Example 1 (distance on 1-D line). The MMSE estimator for the distance $z_k = |x_k - a_k|$ between the moving point (x_k) and given sequence (a_k) in 1-D line takes the form

$$\begin{aligned} \hat{z}_k^{\text{opt}} &= \sqrt{\frac{2P_k}{\pi}} \exp\left[-\frac{(\hat{x}_k - a_k)^2}{2P_k}\right] \\ &+ (\hat{x}_k - a_k) \left[1 - 2\Phi\left(-\frac{(\hat{x}_k - a_k)}{\sqrt{P_k}}\right)\right]. \end{aligned} \quad (11)$$

Example 2 (distance between point and line). The shortest distance $d_k(\mathcal{L}, M)$ from the moving point $M(\mathbf{x}_k) = M(x_{1,k}, x_{2,k})$ to the line $\mathcal{L}: Ax_1 + Bx_2 + C = 0$ in 2-D plane is shown in Figure 2. The distance is given by

$$d_k(\mathcal{L}, M) = \frac{|Ax_{1,k} + Bx_{2,k} + C|}{\sqrt{A^2 + B^2}}. \quad (12)$$

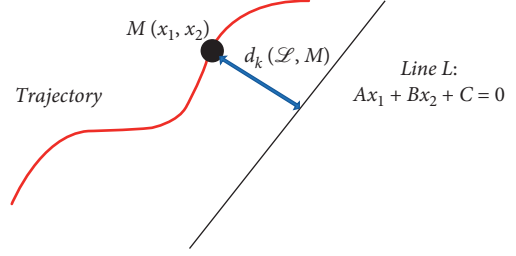


FIGURE 2: Shortest distance $d_k(\mathcal{L}, M)$ from moving point $M(x_k)$ to 1-D line.

Substituting $\mathbf{c}^T = [A \ B]$ and $d = C$ into equations (9) and (10), we get the MMSE estimator for the shortest distance (12):

$$\begin{aligned} \hat{d}_k^{\text{opt}}(\mathcal{L}, M) &= \frac{1}{\sqrt{A^2 + B^2}} \left\{ \sqrt{\frac{2P_k^{(\ell)}}{\pi}} \exp\left(-\frac{\hat{\ell}_k^2}{2P_k^{(\ell)}}\right) \right. \\ &\left. + \hat{\ell}_k \left[1 - 2\Phi\left(-\frac{\hat{\ell}_k}{\sqrt{P_k^{(\ell)}}}\right)\right] \right\}, \end{aligned} \quad (13)$$

where $\hat{\ell}_k$ and $P_k^{(\ell)}$ are determined by equation (9):

$$\begin{aligned} \hat{\ell}_k &= A\hat{x}_{1,k} + B\hat{x}_{2,k} + C, \\ P_k^{(\ell)} &= A^2 P_{11,k} + B^2 P_{22,k} + 2ABP_{12,k}. \end{aligned} \quad (14)$$

The MMSE estimator (12)–(14) can be generalized on 3-D space.

Example 3 (distance between point and plane). Similar to equation (12), the shortest distance between the moving point $M(\mathbf{x}_k) = M(x_{1,k}, x_{2,k}, x_{3,k})$ and the plane $\mathcal{P}: Ax_1 + Bx_2 + Cx_3 + D = 0$ in 3-D space,

$$d_k(\mathcal{P}, M) = \frac{|Ax_{1,k} + Bx_{2,k} + Cx_{3,k} + D|}{\sqrt{A^2 + B^2 + C^2}}, \quad (15)$$

is shown in Figure 3.

Substituting $\mathbf{c}^T = [A \ B \ C]$ and $d = D$ into equations (9) and (10), we get

$$\begin{aligned} \hat{d}_k^{\text{opt}}(\mathcal{P}, M) &= \frac{1}{\sqrt{A^2 + B^2 + C^2}} \left\{ \sqrt{\frac{2P_k^{(\ell)}}{\pi}} \exp\left(-\frac{\hat{\ell}_k^2}{2P_k^{(\ell)}}\right) \right. \\ &\left. + \hat{\ell}_k \left[1 - 2\Phi\left(-\frac{\hat{\ell}_k}{\sqrt{P_k^{(\ell)}}}\right)\right] \right\}, \end{aligned} \quad (16)$$

where $\hat{\ell}_k$ and $P_k^{(\ell)}$ are determined by equation (9):

$$\begin{aligned} \hat{\ell}_k &= A\hat{x}_{1,k} + B\hat{x}_{2,k} + C\hat{x}_{3,k} + D, \\ P_k^{(\ell)} &= A^2 P_{11,k} + B^2 P_{22,k} + C^2 P_{33,k} \\ &+ 2AP_{12,k} + 2ACP_{13,k} + 2BCP_{23,k}. \end{aligned} \quad (17)$$

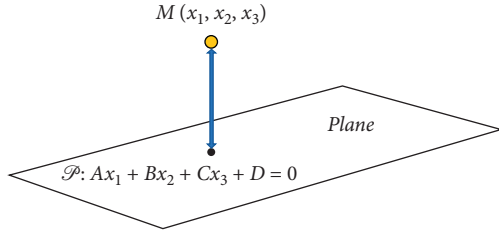


FIGURE 3: Shortest distance from point $M(x_1, x_2, x_3)$ to a plane in 3-D.

The MMSE distance estimators in Theorem 1 and Examples 1~3 are summarized in Table 2.

4.3. Numerical Examples. In this section, numerical examples demonstrate the accuracy of the two closed-form estimators calculated for the absolute value $z = |\mathbf{c}^T \mathbf{x}|$. The optimal MMSE estimator \hat{z}^{opt} is compared with the *simple suboptimal* one $\hat{z}^{\text{sub}} = |\mathbf{c}^T \hat{\mathbf{x}}|$.

4.3.1. Estimation of Distance between Random Location and Given Point in 1-D Line. Let x_k be a scalar random position measured in additive white noise; then, the system model is

$$\begin{aligned} x_{k+1} &= x_k + v_k, & x_0 &= m_0, \\ y_k &= x_k + w_k, & k &= 1, 2, \dots, \end{aligned} \quad (18)$$

where m_0 is the known initial condition and $v_k \sim \mathbb{N}(0, q)$ and $w_k \sim \mathbb{N}(0, r)$ are the uncorrelated white Gaussian noises.

The KF equation (3) gives the following:

$$\begin{aligned} \hat{x}_{k+1} &= \hat{x}_k + K_{k+1}(y_{k+1} - \hat{x}_k), \\ P_{k+1}^- &= P_k + q, P_0 = \sigma_0^2 = 1, K_{k+1} = \frac{P_{k+1}^-}{r + P_{k+1}^-}, \end{aligned} \quad (19)$$

$$P_{k+1} = (1 - K_{k+1})P_{k+1}^-, \quad k = 0, 1, \dots$$

Consider the distance between x_k and the known point a , i.e., $z_k = |x_k - a|$. Then, the optimal MMSE estimate of the distance is defined by (10). Further we are interested in the special case in which $a = 0$ and $z_k = |x_k|$. In this case, formula (10) represents the optimal estimate of the distance between the current position x_k and the origin point, i.e.,

$$\begin{aligned} \hat{z}_k^{\text{opt}} &= \sqrt{\frac{2P_k}{\pi}} \exp(-\alpha_k) + \hat{x}_k [1 - 2\Phi(-\beta_k)], \\ \alpha_k &= \frac{\hat{x}_k^2}{(2P_k)}, \\ \beta_k &= \frac{\hat{x}_k}{\sqrt{P_k}}. \end{aligned} \quad (20)$$

In parallel to the optimal estimate (20), consider the simple suboptimal estimate, $\hat{z}_k^{\text{sub}} = |\hat{x}_k|$.

Remark 2. Reviewing formula (20), we find the following. If the values of α_k and β_k are large ($\alpha_k, |\beta_k| \gg 1$), then $\exp(-\alpha_k) \approx 0$ and $\Phi(-\beta_k) \approx 0$ if $\hat{x}_k > 0$ or $\Phi(-\beta_k) \approx 1$ if $\hat{x}_k < 0$, which implies that both estimates are quite close, i.e., $\hat{z}_k^{\text{opt}} \approx \hat{z}_k^{\text{sub}} = |\hat{x}_k|$. Assuming the estimate \hat{x}_k is far enough from zero, then the large values of the functions α_k and β_k depend on the error variance P_k . Using (19), the steady-state value of the variance P_∞ satisfies the quadratic equation $P_\infty^2 + qP_\infty - rq = 0$ with solution $P_\infty = (-q + \sqrt{q^2 + 4rq})/2$. Since the variance $P_\infty = P_\infty(q, r)$ depends on the noise statistics q and r , this fact can be used in practice to compare the proposed estimators. For example, if the estimate \hat{x}_k is far enough from zero and the product rq is small ($rq \ll 1$), then $P_\infty \approx 0$, and $\alpha_k, |\beta_k| \gg 1$. In this case, both estimators are close, $\hat{z}_k^{\text{opt}} \approx \hat{z}_k^{\text{sub}}$. Simulation results confirm this result.

Next, we test the efficiency of the proposed estimators. The estimators are compared under different values of the noise variances q and r . The following scenarios were considered:

Case 1: small noises, $q = 10^{-4}, r = 10^{-2}$

Case 2: medium noises, $q = 0.1, r = 0.5$

Case 3: large noises, $q = 0.5, r = 1$

Both estimators were run with the same random noises for further comparison. The Monte Carlo simulation with 1000 runs was applied in calculation of the root mean square error (RMSE), $\text{RMSE}_k^{\text{opt}} = \sqrt{\mathbb{E}(z_k - \hat{z}_k^{\text{opt}})^2}$, and $\text{RMSE}_k^{\text{sub}} = \sqrt{\mathbb{E}(z_k - \hat{z}_k^{\text{sub}})^2}$. Define the average RMSE over the time interval $k \in [k_1, k_2]$ as

$$\bar{R}(\hat{z}) \stackrel{\text{def}}{=} \frac{1}{k_2 - k_1 + 1} \sum_{k=k_1}^{k_2} \text{RMSE}_k. \quad (21)$$

The simulation results are illustrated in Table 3 and Figures 4~7.

In Case 1, interest is zero and nonzero initial condition $x_0 = m_0$.

At $m_0 = 0$ and $q = 10^{-4}$, the signal x_k and its estimate \hat{x}_k are close to zero, and $P_k \approx 0.001$ at $k > 8$. In this case, the values of α_k and β_k are not large; therefore, the optimal and suboptimal estimates are different as shown in Figure 4 and confirmed by the values $\bar{R}(\hat{z}^{\text{opt}}) = 0.0213$ and $\bar{R}(\hat{z}^{\text{sub}}) = 0.0327$ in Table 3.

At $m_0 = 1$ and $q = 10^{-4}$, the estimate \hat{x}_k is far enough from zero, and $P_k \approx 0.001$. According to Remark 1, the optimal and suboptimal estimates are approximately equal, $\hat{z}_k^{\text{opt}} \approx \hat{z}_k^{\text{sub}}$, as shown in Figure 5. The equal values $\bar{R}(\hat{z}^{\text{opt}}) = \bar{R}(\hat{z}^{\text{sub}}) = 0.0334$ confirm the fact.

In Cases 2 and 3, the variance P_∞ is not small; therefore, the initial condition m_0 does not play a significant role in comparing both estimators. In these cases, the optimal estimator \hat{z}_k^{opt} has better performance than the simple suboptimal one $\hat{z}_k^{\text{sub}} = |\hat{x}_k|$. Typical graphics are shown in Figures 6 and 7, and the values $\bar{R}(\hat{z}^{\text{opt}})$ and $\bar{R}(\hat{z}^{\text{sub}})$ in Table 3 confirm that conclusion.

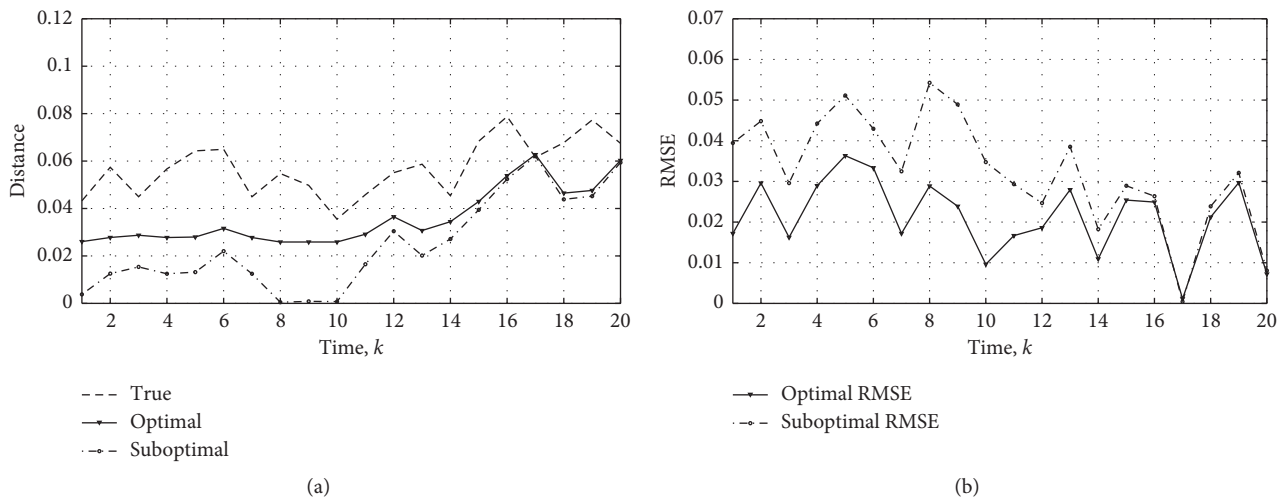
Thus, the simulation results in Section 4.3.1 show that the optimal estimator is suitable for practical applications.

TABLE 2: MMSE estimators for distance in the Cartesian coordinates.

Definition of distance	MMSE distance estimator	Equation
Absolute value $z = x $	$\hat{z}^{\text{opt}} = \Gamma(\hat{x}, P),$ $\Gamma(\hat{x}, P) = \sqrt{2P/\pi} \exp(-\hat{x}^2/2P) + \hat{x}[1 - 2\Phi(-\hat{x}/\sqrt{P})].$	(8)
Absolute value of linear form $z = \mathbf{c}^T \mathbf{x} + d $	$\hat{z}^{\text{opt}} = \Gamma_1(\hat{\ell}, P^{(\ell)}),$ $\Gamma_1(\hat{\ell}, P^{(\ell)}) = \sqrt{2P^{(\ell)}/\pi} \exp(-\hat{\ell}^2/2P^{(\ell)}) + \hat{\ell}[1 - 2\Phi(-\hat{\ell}/\sqrt{P^{(\ell)}})],$ $\hat{\ell} = \mathbf{c}^T \hat{\mathbf{x}} + d, \quad P^{(\ell)} = \mathbf{c}^T \mathbf{P} \mathbf{c}$	(9) and (10)
Distance between two points on 1-D line $z = x - a $	$\hat{z}^{\text{opt}} = \Gamma_1(\hat{\ell}, P),$ $\hat{\ell} = \hat{x} - a$	(11)
Distance between point M and line \mathcal{L} in 2-D plane $d(\mathcal{L}, M) = Ax_1 + Bx_2 + C /\sqrt{A^2 + B^2}$	$\hat{d}(\mathcal{L}, M) = (1/\sqrt{A^2 + B^2})\Gamma_1(\hat{\ell}, P^{(\ell)}),$ $\hat{\ell} = A\hat{x}_1 + B\hat{x}_2 + C,$ $P^{(\ell)} = A^2P_{11} + B^2P_{22} + 2ABP_{12}$	(12)-(14)
Distance between point M and plane \mathcal{P} in 3-D space $d(\mathcal{P}, M) = Ax_1 + Bx_2 + Cx_3 + D /\sqrt{A^2 + B^2 + C^2}$	$\hat{d}(\mathcal{P}, M) = (1/\sqrt{A^2 + B^2 + C^2})\Gamma_1(\hat{\ell}, P^{(\ell)}),$ $\hat{\ell} = A\hat{x}_1 + B\hat{x}_2 + C\hat{x}_3 + D,$ $P^{(\ell)} = A^2P_{11} + B^2P_{22} + C^2P_{33} + 2ABP_{12} + 2ACP_{13} + 2BCP_{23}$	(15)-(17)

TABLE 3: Simulation results for Section 4.3.1.

Case 1: small noises	$q = 0.0001$	$m_0 = 0$	$\bar{R}(\hat{z}^{\text{opt}}) = 0.0213$	$\bar{R}(\hat{z}^{\text{sub}}) = 0.0327$	Figures 4(a) and 4(b)
	$r = 0.001$	$m_0 = 1$	$\bar{R}(\hat{z}^{\text{opt}}) = 0.0334$	$\bar{R}(\hat{z}^{\text{sub}}) = 0.0334$	Figures 5(a) and 5(b)
	$P_\infty \approx 0.001$				
Case 2: medium noises	$q = 0.1$	$m_0 = 0$	$\bar{R}(\hat{z}^{\text{opt}}) = 0.3110$	$\bar{R}(\hat{z}^{\text{sub}}) = 0.3883$	Figures 6(a) and 6(b)
	$r = 0.5$	$m_0 = 1$	$\bar{R}(\hat{z}^{\text{opt}}) = 0.3047$	$\bar{R}(\hat{z}^{\text{sub}}) = 0.3201$	
	$P_\infty \approx 0.18$				
Case 3: large noises	$q = 0.5$	$m_0 = 0$	$\bar{R}(\hat{z}^{\text{opt}}) = 0.6296$	$\bar{R}(\hat{z}^{\text{sub}}) = 0.6991$	Figures 7(a) and 7(b)
	$r = 1$	$m_0 = 1$	$\bar{R}(\hat{z}^{\text{opt}}) = 0.5359$	$\bar{R}(\hat{z}^{\text{sub}}) = 0.5798$	
	$P_\infty \approx 0.5$				

FIGURE 4: Comparison between optimal and suboptimal estimators for small noises (Case 1) with $q = 0.0001$, $r = 0.01$, $P_\infty \approx 0.001$, and zero initial condition $m_0 = 0$. (a) True and estimated values for $z_k = |x_k|$. (b) RMSEs for both estimators.

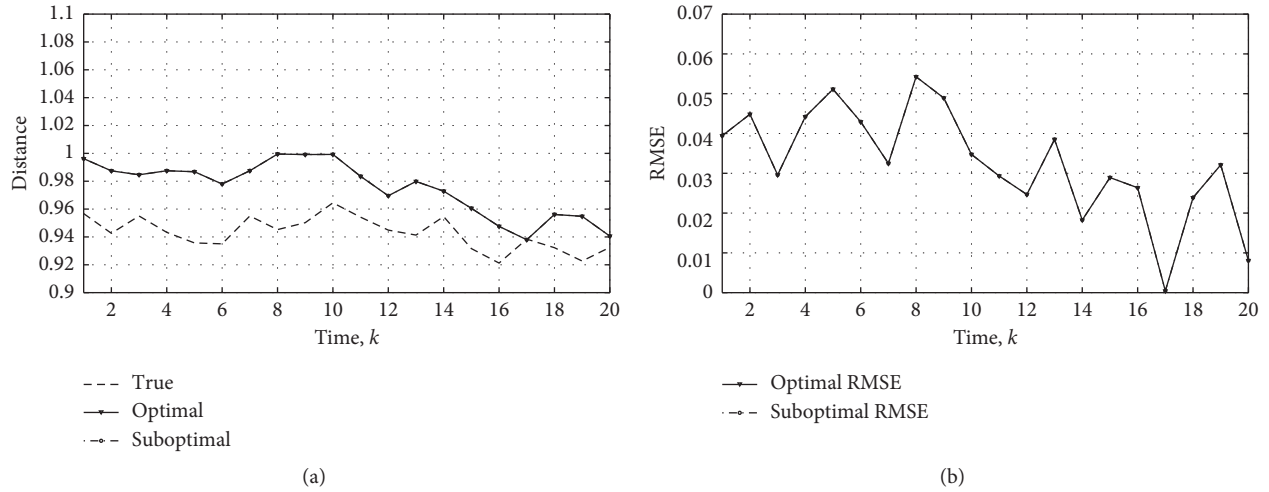


FIGURE 5: Comparison between optimal and suboptimal estimators for small noises (Case 1) with $q = 0.0001$, $r = 0.01$, $P_\infty = 0.001$, and nonzero initial condition $m_0 = 1$. (a) True and very close estimates for $z_k = |x_k|$. (b) Very close RMSE values for both estimators.

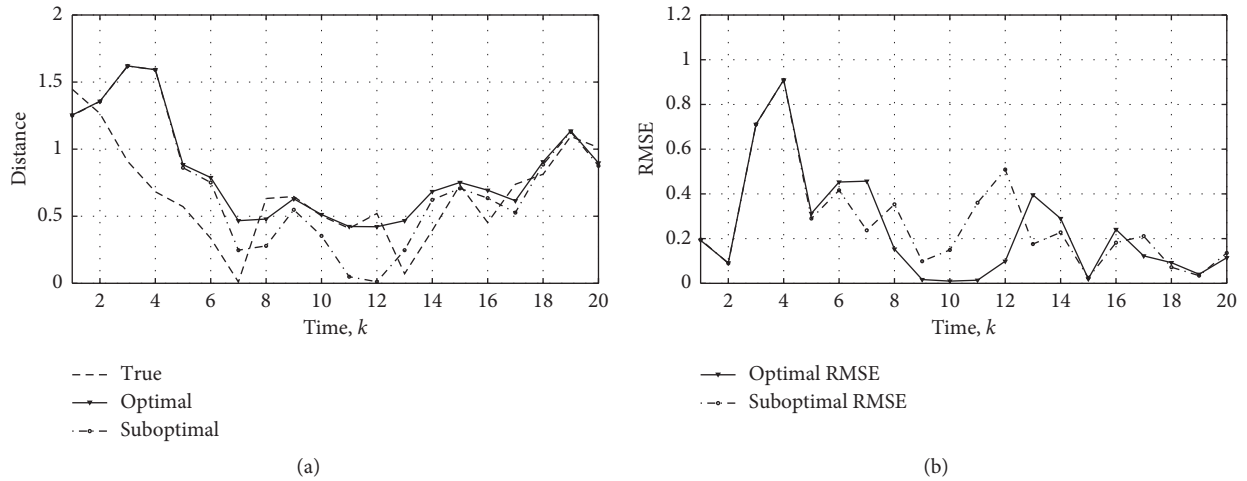


FIGURE 6: Comparison between optimal and suboptimal estimators for medium noises (Case 2) with $q = 0.1$, $r = 0.5$, $P_\infty = 0.18$, and zero initial condition $m_0 = 0$. (a) True and estimated values for $z_k = |x_k|$. (b) RMSEs for both estimators.

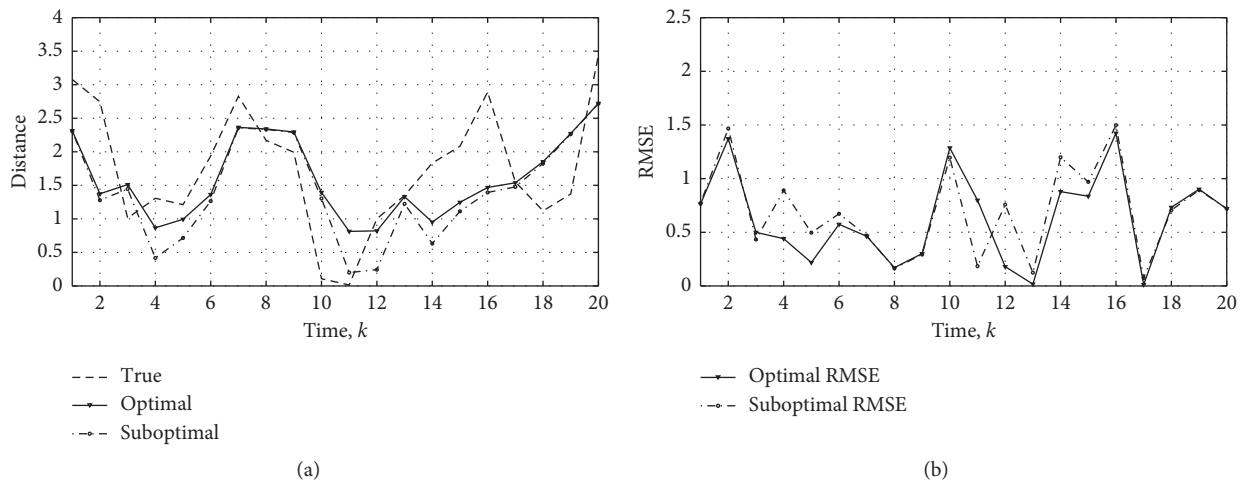


FIGURE 7: Comparison between optimal and suboptimal estimators for large noises (Case 3) with $q = 0.5$, $r = 1.0$, $P_\infty = 0.5$, and zero initial condition $m_0 = 0$. (a) True and estimated values for $z_k = |x_k|$. (b) RMSEs for both estimators.

4.3.2. Estimation of Distance between Two Random Points in 1-D Line. Consider a motion of two random points $A_1(x_1)$ and $A_2(x_2)$ in 1-D line. Assume that evolution of the state vector $\mathbf{x}_k = [x_{1,k} \ x_{2,k}]^T$ from time t_k to t_{k+1} is defined by the random walk model:

$$\begin{aligned} x_{1,k+1} &= x_{1,k} + v_{1,k}, \quad x_{1,0} = m_1, \quad k = 0, 1, \dots, \\ x_{2,k+1} &= x_{2,k} + v_{2,k}, \quad x_{2,0} = m_2, \end{aligned} \quad (22)$$

where m_1 and m_2 are the known initial conditions and $v_{1,k} \sim \mathbb{N}(0, q_1)$ and $v_{2,k} \sim \mathbb{N}(0, q_2)$ are uncorrelated white Gaussian noises.

Assuming we measure the true position of the points with correlated measurement white noises w_1 and w_2 , respectively, the measurement equation is

$$\begin{aligned} y_{1,k} &= x_{1,k} + w_{1,k}, \quad w_{1,k} \sim \mathbb{N}(0, r_1), \\ y_{2,k} &= x_{2,k} + w_{2,k}, \quad w_{2,k} \sim \mathbb{N}(0, r_2), \end{aligned} \quad (23)$$

where $\mathbb{E}(w_{1,k}w_{2,k}) = r_{12}$.

Our goal is to estimate the unknown distance $d(A_1, A_2) = |x_{1,k} - x_{2,k}|$ between the current location of the points $A_1(x_{1,k})$ and $A_2(x_{2,k})$.

According to the proposed two-step estimation procedure, the optimal Kalman estimate $\hat{\mathbf{x}}_k = [\hat{x}_{1,k} \ \hat{x}_{2,k}]^T$ and error covariance $\mathbf{P}_k = [P_{ij,k}]$, $\mathbf{P}_0 = \mathbf{I}_2$ computed at the first stage are used at the second stage for estimation of the distance $z_k = |x_{1,k} - x_{2,k}|$. Using formulas (9) and (10) for $\mathbf{c}^T = [1 \ -1]$ and $d = 0$, we obtain the best MMSE estimate for the distance:

$$\begin{aligned} \hat{z}_k^{\text{opt}} &= \sqrt{\frac{2P_k^{(\ell)}}{\pi}} \exp(-\alpha_k) + \hat{\ell}_k [1 - 2\Phi(-\beta_k)], \\ \alpha_k &= \frac{\hat{\ell}_k^2}{2P_k^{(\ell)}}, \\ \beta_k &= \frac{\hat{\ell}_k}{\sqrt{P_k^{(\ell)}}}, \\ \hat{\ell}_k &= \hat{x}_{1,k} - \hat{x}_{2,k}, \\ P_k^{(\ell)} &= P_{11,k} + P_{22,k} - 2P_{12,k}. \end{aligned} \quad (24)$$

In parallel with the optimal distance estimator (24), we consider the simple suboptimal estimator $\hat{z}_k^{\text{sub}} = |\hat{x}_{1,k} - \hat{x}_{2,k}|$.

Remark 3. As we see, the optimal estimate \hat{z}_k^{opt} of the distances in (20) and (24) depends on the functions α_k and β_k . The functions in formulas (20) and (24) are calculated in the pairs of points (\hat{x}_k, P_k) and $(\hat{\ell}_k, P_k^{(\ell)})$, respectively. The second pair depends on the state estimate $\hat{\mathbf{x}}_k = [\hat{x}_{1,k} \ \hat{x}_{2,k}]^T$ and error covariance $\mathbf{P}_k = [P_{ij,k}]$. Therefore, Remark 2 is

also valid for models (22) and (23). For example, if the estimate $\hat{\ell}_k = \hat{x}_{1,k} - \hat{x}_{2,k}$ is far enough from zero and the variance $P_k^{(\ell)} = \mathbb{E}(\ell_k - \hat{\ell}_k)^2$ is small, then $\hat{z}_k^{\text{opt}} \approx \hat{z}_k^{\text{sub}}$. The simulation results in Figure 8 with $P_k^{(\ell)} = 0.0015$, $k > 8$, and very close values of the average RMSEs, $\bar{R}(\hat{z}^{\text{opt}}) = 0.0189$ and $\bar{R}(\hat{z}^{\text{sub}}) = 0.0189$, confirm this fact.

In addition, we are interested in the following new scenarios:

Case 1: both points $A_1(x_1)$ and $A_2(x_2)$ are fixed, and their positions are measured with small noises

Case 2: the first point $A_1(x_1)$ is fixed, but the movement of the second one $A_2(x_2)$ is subject to a small noise

Case 3: the movement of both points is subject to a medium noise

The model parameters and simulation results for the scenarios are illustrated in Table 4. From Table 4, we observe the strong difference between the average RMSEs $\bar{R}(\hat{z}^{\text{opt}})$ and $\bar{R}(\hat{z}^{\text{sub}})$, i.e., $\bar{R}(\hat{z}^{\text{opt}}) < \bar{R}(\hat{z}^{\text{sub}})$. It is not a surprise that the optimal estimator (24) is better than the suboptimal one, $\hat{z}_k^{\text{sub}} = |\hat{x}_{1,k} - \hat{x}_{2,k}|$.

5. MMSE Estimators for Bilinear and Quadratic Forms

5.1. Optimal Closed-Form MMSE Estimator for Quadratic Form. Consider a quadratic form (QF) of the state vector $\mathbf{x}_k \in \mathbb{R}^n$:

$$z_k = \mathbf{x}_k^T \mathbf{A}_k \mathbf{x}_k, \quad \mathbf{A}_k = \mathbf{A}_k^T. \quad (25)$$

In this case, the optimal MMSE estimator (4) can be explicitly calculated in terms of the Kalman estimate $\hat{\mathbf{x}}_k$ and error covariance \mathbf{P}_k .

Theorem 2 (MMSE estimator for QF). *Let $\mathbf{x}_k \in \mathbb{R}^n$ be a normal random vector, and $\hat{\mathbf{x}}_k \in \mathbb{R}^n$ and $\mathbf{P}_k \in \mathbb{R}^{n \times n}$ are the Kalman estimate and error covariance, respectively. Then, the optimal MMSE estimator for the QF $z_k = \mathbf{x}_k^T \mathbf{A}_k \mathbf{x}_k$ has the following closed-form structure:*

$$\hat{z}_k^{\text{opt}} = \hat{\mathbf{x}}_k^T \mathbf{A}_k \hat{\mathbf{x}}_k + \text{tr}(\mathbf{A}_k \mathbf{P}_k). \quad (26)$$

Proof. Using the formulas $\mathbf{x}^T \mathbf{A} \mathbf{x} = \text{tr}(\mathbf{A} \mathbf{x} \mathbf{x}^T)$ and $\mathbb{E}(\mathbf{x} \mathbf{x}^T) = \text{Cov}(\mathbf{x}) + \mathbb{E}(\mathbf{x})\mathbb{E}(\mathbf{x}^T)$, we obtain

$$\begin{aligned} \hat{z}_k^{\text{opt}} &= \mathbb{E}\left(\mathbf{x}_k^T \mathbf{A}_k \mathbf{x}_k \mid \mathbf{y}^k\right) = \mathbb{E}\left(\text{tr}\left(\mathbf{A}_k \mathbf{x}_k \mathbf{x}_k^T\right) \mid \mathbf{y}^k\right) \\ &= \text{tr}\left(\mathbf{A}_k \mathbb{E}\left(\mathbf{x}_k \mathbf{x}_k^T \mid \mathbf{y}^k\right)\right) \\ &= \text{tr}\left(\mathbf{A}_k \left[\mathbf{P}_k + \mathbb{E}\left(\mathbf{x}_k \mid \mathbf{y}^k\right)\mathbb{E}\left(\mathbf{x}_k^T \mid \mathbf{y}^k\right)\right]\right) \\ &= \text{tr}(\mathbf{A}_k \mathbf{P}_k) + \text{tr}\left(\mathbf{A}_k \hat{\mathbf{x}}_k \hat{\mathbf{x}}_k^T\right) = \text{tr}(\mathbf{A}_k \mathbf{P}_k) + \hat{\mathbf{x}}_k^T \mathbf{A}_k \hat{\mathbf{x}}_k. \end{aligned} \quad (27)$$

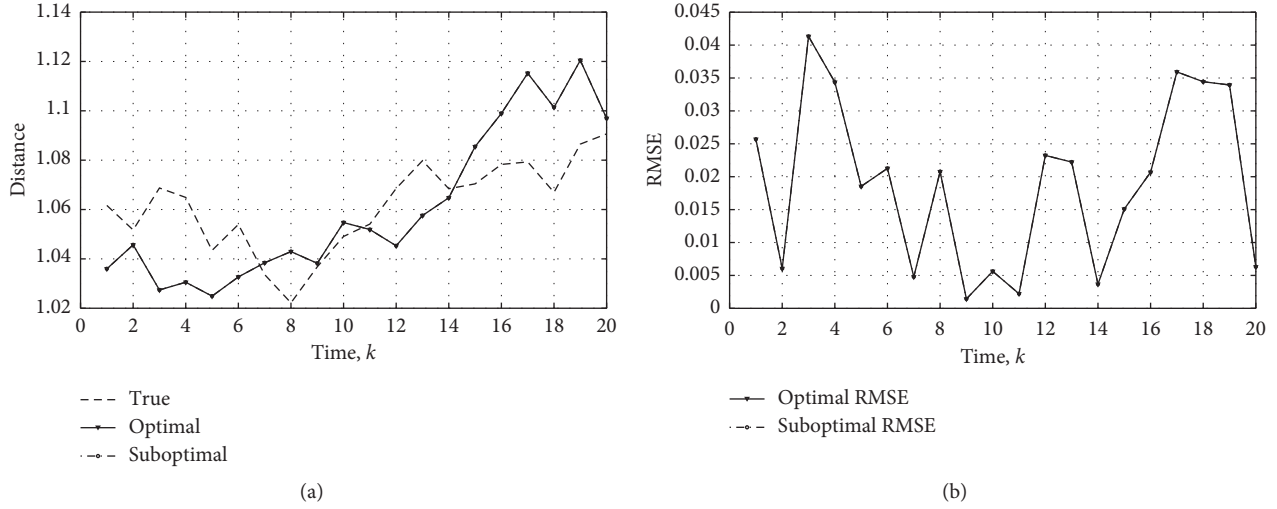


FIGURE 8: Comparison between optimal and suboptimal estimators for small noises with $q_1 = q_2 = 10^{-4}$, $r_1 = r_2 = 10^{-2}$, $r_{12} = 0.005$, and initial positions $m_1 = 0, m_{12} = 1$. (a) True and very close estimates for the distance $z_k = |x_{1,k} - x_{2,k}|$. (b) Very close RMSE values for both estimators.

TABLE 4: Simulation results for Section 4.3.2.

Case 1	$m_1 = 1;$ $m_2 = 1.01$	$q_1 = 0;$ $q_2 = 0$	$r_1 = 0.01;$ $r_2 = 0.01;$ $r_{12} = 0.005$	$P_\infty^{(\ell)} = 0.0001$	$\bar{R}(\hat{z}^{\text{opt}}) = 0.0013$ $\bar{R}(\hat{z}^{\text{sub}}) = 0.0060$
Case 2	$m_1 = 1;$ $m_2 = 1.01$	$q_1 = 0;$ $q_2 = 0.01$	$r_1 = 0.01;$ $r_2 = 0.01;$ $r_{12} = 0.005$	$P_\infty^{(\ell)} = 0.015$	$\bar{R}(\hat{z}^{\text{opt}}) = 0.0378$ $\bar{R}(\hat{z}^{\text{sub}}) = 0.0450$
Case 3	$m_1 = 1;$ $m_2 = 1.01$	$q_1 = 0.05;$ $q_2 = 0.03$	$r_1 = 0.05;$ $r_2 = 0.05;$ $r_{12} = 0.001$	$P_\infty^{(\ell)} = 0.1366$	$\bar{R}(\hat{z}^{\text{opt}}) = 0.1596$ $\bar{R}(\hat{z}^{\text{sub}}) = 0.1796$

In parallel to the optimal quadratic estimator (26), we consider the simple suboptimal estimator denoted as \hat{z}_k^{sub} , which is obtained by direct calculation of the QF at the point $\mathbf{x}_k = \hat{\mathbf{x}}_k$ such as

$$\hat{z}_k^{\text{sub}} = \hat{\mathbf{x}}_k^T \mathbf{A}_k \hat{\mathbf{x}}_k. \quad (28)$$

The simple estimator (28) depends only on the Kalman estimate $\hat{\mathbf{x}}_k$ and does not require the KF error covariance \mathbf{P}_k in contrast to the optimal one (26). The following result compares the estimation accuracy of the optimal and suboptimal quadratic estimators. \square

Lemma 2 (difference between MSEs for quadratic estimators). *The difference between the true MSEs $P_{z,k}^{\text{opt}} = \mathbb{E}(z_k - \hat{z}_k^{\text{opt}})^2$ and $P_{z,k}^{\text{sub}} = \mathbb{E}(z_k - \hat{z}_k^{\text{sub}})^2$ for the optimal and simple suboptimal quadratic estimators is $\text{tr}^2(\mathbf{A}_k \mathbf{P}_k)$.*

Proof. Using the fact that the MMSE estimator is unbiased, $\mathbb{E}(\hat{z}_k^{\text{opt}} - z_k) = 0$, and the equality $\hat{z}_k^{\text{sub}} = \hat{z}_k^{\text{opt}} - \text{tr}(\mathbf{A}_k \mathbf{P}_k)$, we obtain

$$\begin{aligned} P_{z,k}^{\text{sub}} &= \mathbb{E}(z_k - \hat{z}_k^{\text{sub}})^2 \\ &= \mathbb{E}(z_k - \hat{z}_k^{\text{opt}} + \text{tr}(\mathbf{A}_k \mathbf{P}_k))^2 \\ &= \mathbb{E}(z_k - \hat{z}_k^{\text{opt}})^2 + 2\text{tr}(\mathbf{A}_k \mathbf{P}_k) \mathbb{E}(z_k - \hat{z}_k^{\text{opt}}) + \text{tr}^2(\mathbf{A}_k \mathbf{P}_k) \\ &= P_{z,k}^{\text{opt}} + \text{tr}^2(\mathbf{A}_k \mathbf{P}_k). \end{aligned} \quad (29)$$

Let us illustrate Theorem 2 and Lemma 2 on the example of the squared norm of a random vector, $z_k = \|\mathbf{x}_k\|^2 = \mathbf{x}_k^T \mathbf{x}_k$. Then, $\mathbf{A}_k = \mathbf{I}_n$, and the quadratic estimators and difference between their MSEs take the form

$$\begin{aligned} \hat{z}_k^{\text{opt}} &= \hat{\mathbf{x}}_k^T \hat{\mathbf{x}}_k + \text{tr}(\mathbf{P}_k), \\ \hat{z}_k^{\text{sub}} &= \hat{\mathbf{x}}_k^T \hat{\mathbf{x}}_k, \quad \delta_k = P_{z,k}^{\text{sub}} - P_{z,k}^{\text{opt}} = \text{tr}^2(\mathbf{P}_k). \end{aligned} \quad (30)$$

We see the difference $\delta_k = \text{tr}^2(\mathbf{P}_k)$ depends on the quality of the KF data processing (3). \square

5.2. Optimal Closed-Form MMSE Estimator for Bilinear Form. Let $\mathbf{x}_k \in \mathbb{R}^n$ and $\tilde{\mathbf{x}}_k \in \mathbb{R}^n$ be two arbitrary state vectors. Then, a bilinear form (BLF) on the state space can be written as follows:

$$u_k = \mathbf{x}_k^T \mathbf{A}_k \tilde{\mathbf{x}}_k, \quad \mathbf{A}_k = \mathbf{A}_k^T. \quad (31)$$

Note that a BLF can be written as a QF in the vector $\mathbf{X}_k \in \mathbb{R}^{2n}$. In this case,

$$u_k = \mathbf{x}_k^T \mathbf{A}_k \tilde{\mathbf{x}}_k = \begin{bmatrix} \mathbf{x}_k^T & \tilde{\mathbf{x}}_k^T \end{bmatrix} \mathbf{B}_k \begin{bmatrix} \mathbf{x}_k \\ \tilde{\mathbf{x}}_k \end{bmatrix} = \mathbf{X}_k^T \mathbf{B}_k \mathbf{X}_k, \quad (32)$$

$$\mathbf{X}_k = \begin{bmatrix} \mathbf{x}_k \\ \tilde{\mathbf{x}}_k \end{bmatrix},$$

$$\mathbf{X}_k^T = \begin{bmatrix} \mathbf{x}_k^T & \tilde{\mathbf{x}}_k^T \end{bmatrix},$$

$$\mathbf{B}_k = \begin{bmatrix} \mathbf{O}_n & \frac{1}{2} \mathbf{A}_k \\ \frac{1}{2} \mathbf{A}_k^T & \mathbf{O}_n \end{bmatrix}.$$

For the QF (25), the optimal bilinear estimator can be explicitly calculated in terms of the Kalman estimate $\hat{\mathbf{x}}_k \in \mathbb{R}^{2n}$ and block error covariance matrix $\mathbf{P}_k \in \mathbb{R}^{2n \times 2n}$:

$$\hat{\mathbf{x}}_k = \begin{bmatrix} \hat{\mathbf{x}}_k \\ \hat{\tilde{\mathbf{x}}}_k \end{bmatrix}, \quad (33)$$

$$\mathbf{P}_k = \begin{bmatrix} \mathbf{P}_{xx,k} & \mathbf{P}_{x\tilde{x},k} \\ \mathbf{P}_{x\tilde{x},k}^T & \mathbf{P}_{\tilde{x}\tilde{x},k} \end{bmatrix},$$

where $\mathbf{P}_{x\tilde{x},k} = \text{Cov}(\mathbf{e}_{x,k}, \mathbf{e}_{\tilde{x},k})$ is a cross covariance between estimation errors $\mathbf{e}_{x,k} = \mathbf{x}_k - \hat{\mathbf{x}}_k$ and $\mathbf{e}_{\tilde{x},k} = \tilde{\mathbf{x}}_k - \hat{\tilde{\mathbf{x}}}_k$.

Applying Theorem 2 to the QF $z_k = \mathbf{X}_k^T \mathbf{B}_k \mathbf{X}_k$ and taking into consideration the block structure of the matrix \mathbf{B}_k , we have the following.

Theorem 3 (MMSE estimator for BLF). *Let $\mathbf{x}_k = [\mathbf{x}_k^T \tilde{\mathbf{x}}_k^T]^T \in \mathbb{R}^{2n}$ be a joint normal random vector, and $\hat{\mathbf{x}}_k \in \mathbb{R}^{2n}$ and $\mathbf{P}_k \in \mathbb{R}^{2n \times 2n}$ are the Kalman estimate and block error covariance matrix (33). Then, the optimal MMSE estimator for the BLF $u_k = \mathbf{x}_k^T \mathbf{A}_k \tilde{\mathbf{x}}_k$ has the following closed-form structure:*

$$\hat{u}_k^{\text{opt}} = \hat{\mathbf{x}}_k^T \mathbf{A}_k \hat{\tilde{\mathbf{x}}}_k + \text{tr}(\mathbf{A}_k \mathbf{P}_{x\tilde{x},k}). \quad (34)$$

Example 4 (estimation of inner product and squared Euclidean distance). Using the bilinear estimator (34) with $\mathbf{A}_k = \mathbf{I}_n$, the MMSE estimator for the inner product $u_k = \mathbf{x}_k^T \tilde{\mathbf{x}}_k$ takes the form

$$\hat{u}_k^{\text{opt}} = \hat{\mathbf{x}}_k^T \hat{\tilde{\mathbf{x}}}_k + \text{tr}(\mathbf{P}_{x\tilde{x},k}). \quad (35)$$

Next, calculate the optimal MMSE estimator for the squared Euclidean distance between two points $z_k = d^2(\mathbf{x}_k, \tilde{\mathbf{x}}_k) = \|\mathbf{x}_k - \tilde{\mathbf{x}}_k\|_2^2$ or $z_k = \|\eta_k\|_2^2$, where $\eta_k = \mathbf{x}_k - \tilde{\mathbf{x}}_k$. The Kalman estimate and error covariance of the difference η_k take the form

$$\hat{\eta}_k = \hat{\mathbf{x}}_k - \hat{\tilde{\mathbf{x}}}_k, \quad (36)$$

$$\mathbf{P}_k^{(\eta)} = \mathbf{P}_{xx,k} + \mathbf{P}_{x\tilde{x},k} - \mathbf{P}_{x\tilde{x},k} - \mathbf{P}_{x\tilde{x},k}^T.$$

Applying the quadratic estimator (26) with $\mathbf{A}_k = \mathbf{I}_n$, we obtain the MMSE estimator for the squared Euclidean distance:

$$\hat{z}_k^{\text{opt}} = \hat{\eta}_k^T \hat{\eta}_k + \text{tr}(\mathbf{P}_k^{(\eta)}) = (\hat{\mathbf{x}}_k - \hat{\tilde{\mathbf{x}}}_k)^T (\hat{\mathbf{x}}_k - \hat{\tilde{\mathbf{x}}}_k) + \text{tr}(\mathbf{P}_k^{(\eta)}). \quad (37)$$

The MMSE estimators for bilinear and quadratic forms are summarized in Table 5.

5.3. Practical Usefulness of Squared Euclidean Distance. In many practical problems, for example, finding the shortest distance from a point to a curve, $\min_{\mathbf{x}, \tilde{\mathbf{x}} \in \mathcal{M}} d(\mathbf{x}, \tilde{\mathbf{x}})$, or comparing a distance with a threshold value, $d(\mathbf{x}, \tilde{\mathbf{x}}) \geq \varepsilon$, there is no need to calculate the original Euclidean distance $d(\mathbf{x}, \tilde{\mathbf{x}}) = \sqrt{\sum_{i=1}^n (x_i - \tilde{x}_i)^2}$, but we just need to calculate its square due to the equivalence of the problems, $\min_{\mathbf{x}, \tilde{\mathbf{x}} \in \mathcal{M}} d(\mathbf{x}, \tilde{\mathbf{x}}) \Leftrightarrow \min_{\mathbf{x}, \tilde{\mathbf{x}} \in \mathcal{M}} d^2(\mathbf{x}, \tilde{\mathbf{x}})$ or $d(\mathbf{x}, \tilde{\mathbf{x}}) \geq \varepsilon \Leftrightarrow d^2(\mathbf{x}, \tilde{\mathbf{x}}) \geq \varepsilon^2$. In such situations, the optimal quadratic estimator (37) for the squared Euclidean distance, $d^2(\mathbf{x}, \tilde{\mathbf{x}}) = \sum_{i=1}^n (x_i - \tilde{x}_i)^2$, can be successfully used.

Example 5. (deviation of normal and nominal trajectories). Suppose that the piecewise feedback control law U_k^* depends on the difference between a normal (\mathbf{x}_k) and nominal (\mathbf{x}_k^n) trajectories. For example, it is given by

$$U_k^* = \begin{cases} 1, & d(\mathbf{x}_k, \mathbf{x}_k^n) < D, \\ -1, & \text{otherwise,} \end{cases} \quad (38)$$

where $d(\mathbf{x}_k, \mathbf{x}_k^n)$ is the Euclidean distance and D is the distance threshold (see Figure 9).

In view of the above, rewrite the control law in the equivalent form:

$$U_k^* = \begin{cases} 1, & d^2(\mathbf{x}_k, \mathbf{x}_k^n) < D^2, \\ -1, & \text{otherwise,} \end{cases} \quad (39)$$

where $d^2(\mathbf{x}_k, \mathbf{x}_k^n)$ is the squared of the Euclidean distance and D^2 is the new threshold.

Using the quadratic estimator (37) for the squared distance $z_k = d^2(\mathbf{x}_k, \mathbf{x}_k^n)$, we obtain the MMSE estimator, $\hat{z}_k^{\text{opt}} = (\hat{\mathbf{x}}_k - \hat{\mathbf{x}}_k^n)^T (\hat{\mathbf{x}}_k - \hat{\mathbf{x}}_k^n) + \text{tr}(\mathbf{P}_k)$, which can be used in the control (39):

$$U_k^* = \begin{cases} 1, & \hat{z}_k^{\text{opt}} < D^2, \\ -1, & \text{otherwise.} \end{cases} \quad (40)$$

In the next section, we discuss application of the linear, bilinear, and quadratic estimators (Theorems 1–3) for estimation of composite nonlinear functions.

TABLE 5: MMSE estimators for QF, BLF, inner product, and squared norm.

Title	Formula for function	MMSE estimator	Equation
QF	$z = \mathbf{x}^T \mathbf{A} \mathbf{x}, \mathbf{A} = \mathbf{A}^T$	$\hat{z}^{\text{opt}} = \hat{\mathbf{x}}^T \mathbf{A} \hat{\mathbf{x}} + \text{tr}(\mathbf{A} \mathbf{P})$	(26)
BLF	$u = \mathbf{x}^T \mathbf{B} \tilde{\mathbf{x}}, \mathbf{B} = \mathbf{B}^T$	$\hat{u}^{\text{opt}} = \hat{\mathbf{x}}^T \mathbf{B} \hat{\tilde{\mathbf{x}}} + \text{tr}(\mathbf{B} \mathbf{P}_{\tilde{\mathbf{x}}})$	(34)
Inner product	$u = \langle \mathbf{x}, \tilde{\mathbf{x}} \rangle = \mathbf{x}^T \tilde{\mathbf{x}}$	$\hat{u}^{\text{opt}} = \hat{\mathbf{x}}^T \hat{\tilde{\mathbf{x}}} + \text{tr}(\mathbf{P}_{\tilde{\mathbf{x}}})$	(35)
Euclidean distance	$z = \ \mathbf{x} - \tilde{\mathbf{x}}\ _2^2$	$\hat{z}^{\text{opt}} = (\hat{\mathbf{x}} - \hat{\tilde{\mathbf{x}}})^T (\hat{\mathbf{x}} - \hat{\tilde{\mathbf{x}}}) + \text{tr}(\mathbf{P}^{(\eta)}),$ $\mathbf{P}^{(\eta)} = \mathbf{P}_{\mathbf{x}\mathbf{x}} + \mathbf{P}_{\tilde{\mathbf{x}}\tilde{\mathbf{x}}} - \mathbf{P}_{\mathbf{x}\tilde{\mathbf{x}}} - \mathbf{P}_{\tilde{\mathbf{x}}\mathbf{x}}^T$	(37)

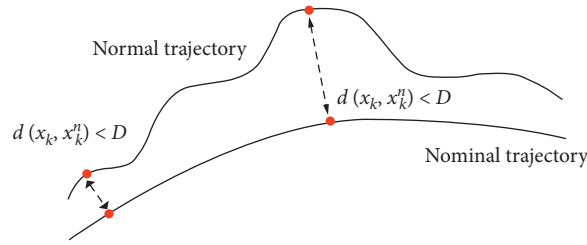


FIGURE 9: Distance deviation between normal and nominal (desired) trajectories.

6. Suboptimal Estimator for Composite Nonlinear Functions

6.1. *Definition of Composite Function.* Consider a composite function F depending on LF, QF, and BLF, such as

$$F(\mathbf{x}) = F(g_1(\mathbf{x}), g_2(\mathbf{x}), \dots, g_h(\mathbf{x})), \quad (41)$$

where the inside functions are defined as

$$g_i(\mathbf{x}) = \begin{cases} \text{LF} = \mathbf{c}^T \mathbf{x}, & \mathbf{x}, \mathbf{c} \in \mathbb{R}^n, \\ \text{QF} = \mathbf{x}^T \mathbf{A} \mathbf{x}, & \mathbf{x} \in \mathbb{R}^n, \mathbf{A} \in \mathbb{R}^{n \times n}, \\ \text{BLF} = \mathbf{x}^T \mathbf{B} \tilde{\mathbf{x}}, & \mathbf{x}, \tilde{\mathbf{x}} \in \mathbb{R}^n, \mathbf{B} \in \mathbb{R}^{n \times n}. \end{cases} \quad (42)$$

Example 6. (composite and inside functions in object tracking). Let $\mathbf{x} \in \mathbb{R}^6$ be an object state vector consisting of the position (p_x, p_y, p_z) and corresponding velocity (v_x, v_y, v_z) components in the Cartesian coordinates (x, y, z) , i.e.,

$$\begin{aligned} \mathbf{x} &= [x_1 \ x_2 \ x_3 \ x_4 \ x_5 \ x_6]^T \\ &= [p_x \ p_y \ p_z \ v_x \ v_y \ v_z]^T. \end{aligned} \quad (43)$$

In the spherical coordinates, we assume that a Doppler radar is located at the origin of the Cartesian coordinates, and it measures the following quantities obtained via nonlinear composite functions $F_i(g_1(\mathbf{x}), \dots, g_h(\mathbf{x}))$ of the state components depending on LF, QF, and BLF:

$$d = \sqrt{p_x^2 + p_y^2 + p_z^2} = F_1(\mathbf{x}),$$

$$F_1(\mathbf{x}) = \sqrt{g_1(\mathbf{x})}, \quad g_1 = x_1^2 + x_2^2 + x_3^2,$$

$$\theta = \tan^{-1}\left(\frac{p_y}{p_x}\right) = F_2(\mathbf{x}),$$

$$F_2(\mathbf{x}) = \tan^{-1}\left(\frac{g_2(\mathbf{x})}{g_3(\mathbf{x})}\right), \quad g_2 = x_2, g_3 = x_1,$$

$$\varphi = \frac{p_z}{\sqrt{p_x^2 + p_y^2}} = F_3(\mathbf{x}), \quad (44)$$

$$F_3(\mathbf{x}) = \frac{g_4(\mathbf{x})}{\sqrt{g_5(\mathbf{x})}}, \quad g_4 = x_3, g_5 = x_1^2 + x_2^2,$$

$$\dot{d} = \frac{p_x v_x + p_y v_y + p_z v_z}{\sqrt{p_x^2 + p_y^2 + p_z^2}} = F_4(\mathbf{x}),$$

$$F_4(\mathbf{x}) = \frac{g_6(\mathbf{x})}{\sqrt{g_1(\mathbf{x})}}, \quad g_6 = x_1 x_4 + x_2 x_5 + x_3 x_6,$$

where d is the range (distance), θ is the bearing angle, φ is the elevation angle, and \dot{d} is the range rate.

6.2. *Suboptimal Estimator for Composite Functions.* Given the Kalman estimate and covariance $(\hat{\mathbf{x}}, \mathbf{P})$, we estimate a quantity obtained via the composite function $F(\mathbf{x}) = F(g_1(\mathbf{x}), \dots, g_h(\mathbf{x}))$. The idea of the algorithm is based on the optimal MMSE estimators for LF, QF, and BLF proposed in equations (10), (26), and (34), respectively. We have

$$\begin{aligned}
\text{For LF } g_i(\mathbf{x}) &= \mathbf{c}^T \mathbf{x}: \quad \hat{g}_i(\hat{\mathbf{x}}, \mathbf{P}) = \mathbf{c}^T \hat{\mathbf{x}}; \\
\text{For QF } g_i(\mathbf{x}) &= \mathbf{x}^T \mathbf{A} \mathbf{x}: \quad \hat{g}_i(\hat{\mathbf{x}}, \mathbf{P}) = \hat{\mathbf{x}}^T \mathbf{A} \hat{\mathbf{x}} + \text{tr}(\mathbf{A} \mathbf{P}); \\
\text{For BLF } g_i(\mathbf{x}) &= \mathbf{x}^T \mathbf{B} \tilde{\mathbf{x}}: \quad \hat{g}_i(\hat{\mathbf{x}}, \mathbf{P}) = \hat{\mathbf{x}}^T \mathbf{B} \tilde{\hat{\mathbf{x}}} + \text{tr}(\mathbf{B} \mathbf{P}_{xx}).
\end{aligned} \quad (45)$$

Replacing the unknown inside functions $g_i(\mathbf{x})$ with the corresponding optimal estimates (45), we obtain the novel suboptimal estimator for the composite function $z = F(g_1, \dots, g_h)$, i.e.,

$$\hat{z}^{\text{comp}} = F(\hat{g}_1(\hat{\mathbf{x}}, \mathbf{P}), \dots, \hat{g}_h(\hat{\mathbf{x}}, \mathbf{P})). \quad (46)$$

Example 7 (estimation of cosine of angle). Let $\mathbf{X} = [\mathbf{x}^T \quad \tilde{\mathbf{x}}^T]^T \in \mathbb{R}^{2n}$ be a joint normal state vector, and

$$\begin{aligned}
\hat{\mathbf{X}} &= \begin{bmatrix} \hat{\mathbf{x}} \\ \tilde{\hat{\mathbf{x}}} \end{bmatrix}, \\
\mathbf{P} &= \begin{bmatrix} \mathbf{P}_{xx} & \mathbf{P}_{x\tilde{x}} \\ \mathbf{P}_{x\tilde{x}}^T & \mathbf{P}_{\tilde{x}\tilde{x}} \end{bmatrix}
\end{aligned} \quad (47)$$

are the Kalman estimate and block error covariance.

The cosine of angle between two vectors $\mathbf{x}, \tilde{\mathbf{x}} \in \mathbb{R}^n$ is equal to

$$\cos(\theta) = \frac{\langle \mathbf{x}, \tilde{\mathbf{x}} \rangle}{\|\mathbf{x}\| \times \|\tilde{\mathbf{x}}\|} = \frac{\langle \mathbf{x}, \tilde{\mathbf{x}} \rangle}{\sqrt{\mathbf{x}^T \mathbf{x}} \times \sqrt{\tilde{\mathbf{x}}^T \tilde{\mathbf{x}}}} \quad (48)$$

We observe the ratio (48) represents the composite function $z = F(\mathbf{x}, \tilde{\mathbf{x}})$ depending on the three inside functions $g_1 = \sqrt{\mathbf{x}^T \mathbf{x}}$, $g_2 = \sqrt{\tilde{\mathbf{x}}^T \tilde{\mathbf{x}}}$, and $g_0 = \langle \tilde{\mathbf{x}}, \mathbf{x} \rangle$:

$$z = \cos(\theta) = \frac{g_0}{\sqrt{g_1} \times \sqrt{g_2}} \quad (49)$$

The optimal MMSE estimators for the inside functions g_0, g_1 , and g_2 are known. Using equation (45), we have

$$\begin{aligned}
\hat{g}_0 &= \hat{\mathbf{x}}^T \tilde{\hat{\mathbf{x}}} + \text{tr}(\mathbf{P}_{x\tilde{x}}), \\
\hat{g}_1 &= \hat{\mathbf{x}}^T \hat{\mathbf{x}} + \text{tr}(\mathbf{P}_{xx}), \\
\hat{g}_2 &= \tilde{\hat{\mathbf{x}}}^T \tilde{\hat{\mathbf{x}}} + \text{tr}(\mathbf{P}_{\tilde{x}\tilde{x}}).
\end{aligned} \quad (50)$$

Replacing the inside functions g_i with their estimates \hat{g}_i , we get the suboptimal estimator for the cosine of angle:

$$\hat{z}^{\text{com}} = \frac{\hat{g}_0}{\sqrt{\hat{g}_1} \sqrt{\hat{g}_2}} = \frac{\hat{\mathbf{x}}^T \tilde{\hat{\mathbf{x}}} + \text{tr}(\mathbf{P}_{xy})}{\sqrt{\hat{\mathbf{x}}^T \hat{\mathbf{x}} + \text{tr}(\mathbf{P}_{xx})} \times \sqrt{\tilde{\hat{\mathbf{x}}}^T \tilde{\hat{\mathbf{x}}} + \text{tr}(\mathbf{P}_{\tilde{x}\tilde{x}})}} \quad (51)$$

Numerical example illustrates the applicability of the all estimators proposed in the paper.

7. Numerical Example: Motion in a Plane

In this section, we estimate the range and the bearing angle in 2-D motion of an object. Because of the difficulties of getting analytical closed-form expressions for the optimal estimators for range and bearing, we apply the simple estimator (\hat{z}^{sim}) and the estimator based on the composite functions (\hat{z}^{com}). In addition, we are interested in the angle between the two state vectors \mathbf{x}_{k-1} and \mathbf{x}_k at time instants t_{k-1} and t_k , respectively, $\varphi_k \stackrel{\text{def}}{=} \angle(\mathbf{x}_{k-1}, \mathbf{x}_k)$.

7.1. Suboptimal Estimators for Range-Angle Response. The example of Section 4.3.2 is considered again. Consider the 2-D models (22) and (23) describing motion of the two random points $A_1(x_{1,k})$ and $A_2(x_{2,k})$. To calculate the range (d_k), tangent of the bearing angle (θ_k), and cosine of the angle (φ_k), we use the following formulas:

$$\begin{aligned}
f(\mathbf{x}_k) &\stackrel{\text{def}}{=} d_k = \sqrt{x_{1,k}^2 + x_{2,k}^2}, \\
h(\mathbf{x}_k) &\stackrel{\text{def}}{=} \tan(\theta_k) = \frac{x_{2,k}}{x_{1,k}}, \\
g(\mathbf{x}_k) &\stackrel{\text{def}}{=} \cos(\varphi_k) = \frac{\langle \mathbf{x}_{k-1}, \mathbf{x}_k \rangle}{\|\mathbf{x}_{k-1}\| \times \|\mathbf{x}_k\|} \\
&= \frac{x_{1,k-1}x_{1,k} + x_{2,k-1}x_{2,k}}{\sqrt{x_{1,k-1}^2 + x_{2,k-1}^2} \times \sqrt{x_{1,k}^2 + x_{2,k}^2}}
\end{aligned} \quad (52)$$

The following estimators for the range-angle responses (52) are illustrated and compared:

(1) Simple estimator:

$$\begin{aligned}
(a) \hat{f}_k^{\text{sim}} &= \sqrt{\hat{x}_{1,k}^2 + \hat{x}_{2,k}^2}, \\
(b) \hat{h}_k^{\text{sim}} &= \frac{\hat{x}_{2,k}}{\hat{x}_{1,k}}, \\
(c) \hat{g}_k^{\text{sim}} &= \frac{\hat{x}_{1,k-1}\hat{x}_{1,k} + \hat{x}_{2,k-1}\hat{x}_{2,k}}{\sqrt{\hat{x}_{1,k-1}^2 + \hat{x}_{2,k-1}^2} \times \sqrt{\hat{x}_{1,k}^2 + \hat{x}_{2,k}^2}}
\end{aligned} \quad (53)$$

(2) Estimator for composite functions:

$$\begin{aligned}
(a) \hat{f}_k^{\text{com}} &= \sqrt{(\hat{x}_{1,k}^2 + P_{11,k}) + (\hat{x}_{2,k}^2 + P_{22,k})}, \\
(b) \hat{h}_k^{\text{com}} &= \hat{h}_k^{\text{sim}}, \\
(c) \hat{g}_k^{\text{com}} &= \frac{\hat{x}_{1,k-1}\hat{x}_{1,k} + \hat{x}_{2,k-1}\hat{x}_{2,k} + P_{k-1,k}^{(1)} + P_{k-1,k}^{(2)}}{\sqrt{(\hat{x}_{1,k-1}^2 + P_{11,k-1}) + (\hat{x}_{2,k-1}^2 + P_{22,k-1})} \times \sqrt{(\hat{x}_{1,k}^2 + P_{11,k}) + (\hat{x}_{2,k}^2 + P_{22,k})}}
\end{aligned} \quad (54)$$

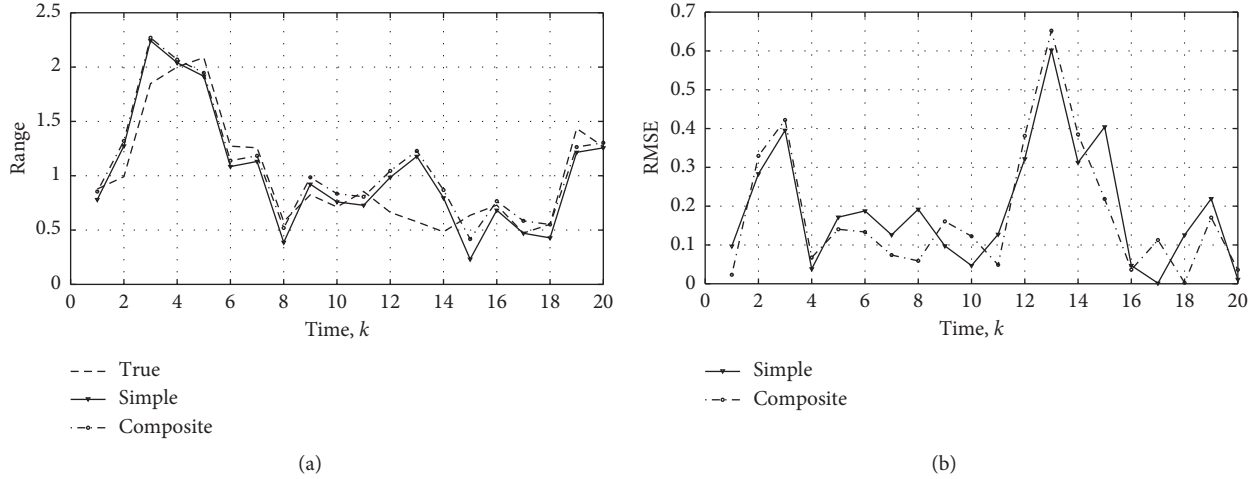


FIGURE 10: Comparison of composite and simple estimators for range. (a) True and estimated ranges. (b) RMSE for both estimators.

Note that the simple and composite estimates \hat{h}_k^{sim} and \hat{h}_k^{com} for a bearing angle coincide. In equation (54), $\hat{P}_{k-1,k}^{(1)} = \mathbb{E}(e_{1,k-1}e_{1,k})$ and $\hat{P}_{k-1,k}^{(2)} = \mathbb{E}(e_{2,k-1}e_{2,k})$ are the error cross-covariances satisfying the following recursive:

$$\begin{aligned} P_{k-1,k}^{(i)} &= (1 - K_k^{(i)})(1 - K_{k-1}^{(i)})P_{k-2,k-1}^{(i)}, \quad k \geq 2, \\ P_{0,1}^{(i)} &= (1 - K_k^{(i)})\sigma_i^2, \quad \sigma_i^2 = \text{Cov}(x_{i,0}), \quad i = 1, 2. \end{aligned} \quad (55)$$

In equations (53)–(55), the values $\hat{x}_{i,k}$, $K_k^{(i)}$, and $P_{ii,k} = \mathbb{E}(e_{i,k}^2)$ represent the Kalman estimate, KF gain, and variance of the error $e_{i,k} = x_{i,k} - \hat{x}_{i,k}$, respectively.

7.2. Simulation Results. The simple and composite estimators were run with the same random noises for further comparison. The Monte Carlo simulation with 1000 runs was applied in calculation of the RMSEs for the range (d_k), the bearing angle (θ_k), and the angle between state vectors (φ_k). Figures 10–12 show the range and angle estimates for the model parameters in equations (22) and (23), with $m_1 = 0.1$, $m_2 = -0.1$, $\mathbf{P}_0 = \mathbf{I}_2$, $q_1 = 0.2$, $q_2 = 0.3$, $r_1 = 0.05$, $r_2 = 0.1$, and $r_{12} = 0$. The following results about the relative performance of the above estimators can be made.

Figure 10(a) presents the range estimators (\hat{f}_k^{sim} , \hat{f}_k^{com}) as well as the true range d_k . Figure 10(b) shows the comparison of the RMSEs for the range estimators. Comparing $\overline{R}(\hat{f}_k^{\text{com}})$ and $\overline{R}(\hat{f}_k^{\text{sim}})$ on the interval $k \in [1; 20]$, we obtain the values 0.0296 and 0.0541, respectively. From Figures 10(a) and 10(b), the range estimator \hat{f}_k^{com} has the better performance compared to the simple one \hat{f}_k^{sim} . This is due to the fact that the MMSE estimate $\hat{z}_k^{\text{opt}} = (\hat{x}_{1,k}^2 + P_{11,k}) + (\hat{x}_{2,k}^2 + P_{22,k})$ of the squared norm $z_k = \|\mathbf{x}_k\|^2 = x_{1,k}^2 + x_{2,k}^2$ contains the error variances $P_{11,k}$ and $P_{22,k}$ as additional terms. If the variances tend to zero, $P_{ii,k} \rightarrow 0$, then the range estimators will converge, i.e., $\hat{f}_k^{\text{com}} \approx \hat{f}_k^{\text{sim}}$.

(2) Figure 11 shows the true value of tangent of the bearing angle $h(x_k) = x_{2,k}/x_{1,k}$ and the

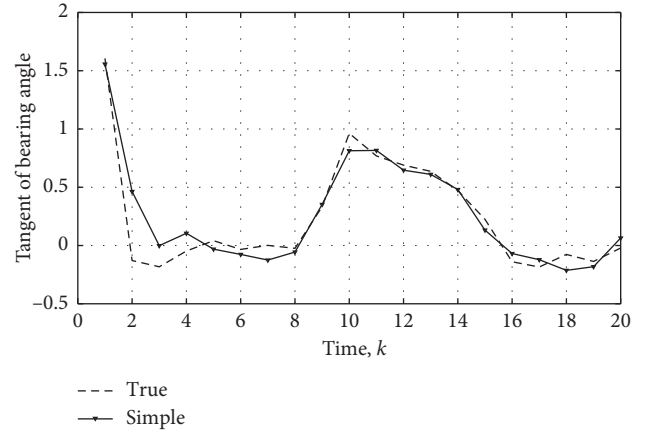


FIGURE 11: True tangent of bearing angle and its simple (composite) estimate.

corresponding simple (or composite) estimate, $\hat{h}_k^{\text{sim}} = \hat{h}_k^{\text{com}} = \hat{x}_{2,k}/\hat{x}_{1,k}$. We observe the negligible difference between the true tangent value $h(x_k)$ and its simple estimate \hat{h}_k^{sim} . The average RMSE of the estimate over the time interval $[1, 20]$ is $\overline{R}(\hat{h}_k^{\text{sim}}) = 0.0672$. It demonstrates reasonable accuracy of the estimator $\hat{x}_{2,k}/\hat{x}_{1,k}$ for the unknown ratio (tangent of angle) $\hat{x}_{2,k}/\hat{x}_{1,k}$.

(3) Similar simulation procedures, as in (1) and (2), were used to check performance of the estimators \hat{g}_k^{sim} and \hat{g}_k^{com} . The true cosine value g_k is shown in Figure 12 for comparison with the estimated values.

For detailed consideration of the proposed estimators, we divide the whole time interval into two subintervals $I_1 = [1; 6]$ and $I_2 = [7; 20]$, respectively. From Figure 12, we can observe that on the first subinterval, the estimate \hat{g}_k^{com} is better than \hat{g}_k^{sim} , and on the second one, the difference between them is negligible. This is also confirmed by the values of $\overline{R}(\hat{g}_k)$ presented in Table 6.

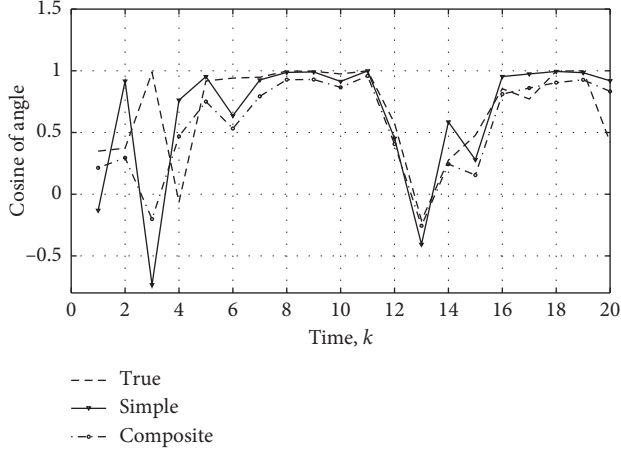


FIGURE 12: True cosine of angle and simple and composite estimates.

TABLE 6: Comparisons of average RMSE for the simple and composite estimators.

	$\bar{R}(\hat{g}_k^{\text{sim}})$	$\bar{R}(\hat{g}_k^{\text{com}})$
$I_1 = [1; 6]$	0.6519	0.4886
$I_2 = [7; 20]$	0.1244	0.1226

Note that both estimators \hat{g}_k^{sim} and \hat{g}_k^{com} are based on the MMSE estimators for a squared norm and inner product. Therefore, the difference between them becomes small if the KF error variances $P_{ii,k}$ are small (see (c) in equations (53) and (54)). In our case, the steady-state values of the variances are $P_{11,k} = 0.0214$ and $P_{22,k} = 0.0101, k > 8$.

8. Conclusion

In this paper, we propose a novel MMSE approach for the estimation of distance metrics under the Kalman filtering framework. The main contributions of the paper are listed in the following.

Firstly, an optimal two-stage MMSE estimator for an arbitrary nonlinear function of a state vector is proposed. The distance metric is an important practical case of such nonlinearities, detailed study of which is given in the paper. Implementation of the MMSE estimator is reduced to calculation of the multivariate Gaussian integral. To avoid the difficulties associated with its calculation, the concept of a closed-form estimator depending on the Kalman filter statistics is introduced. We establish relations between the Euclidean metrics and the closed-form estimator, which lead to simple compact formulas for the real-life distances between points presented in Table 2.

Secondly, an important class of bilinear and quadratic estimators is comprehensively studied. These estimators are applied to a square of norm, Euclidean distance, and inner product. Table 5 summarizes the results. Moreover, an

effective low-complexity suboptimal estimator for nonlinear composite functions is developed using the MMSE bilinear and quadratic estimators. As shown in Section 6.1, radar tracking range-angle responses are described by the composite functions.

Simulation and experimental results show that the proposed estimators perform significantly better than the existing suboptimal distance or angle estimators such as a simple estimator defined in the paper. The low-complexity estimator developed in Section 6.1 is quite promising for radar data processing. Also, the numerical results confirm the fact that the more accurate the Kalman estimate of a state vector, the more accurately we can obtain the range and angle estimates.

Appendix

Proof of Lemma 1. The derivation of formula (8): direct calculation of the Gaussian integral gives

$$\begin{aligned} \mathbb{E}(|x| | y^k) &= \frac{1}{\sqrt{2\pi P}} \int_{-\infty}^{\infty} |x| e^{-(x-\hat{x})^2/2P} dx \\ &= \underbrace{1/\sqrt{2\pi P} \int_0^{\infty} x e^{-(x-\hat{x})^2/2P} dx}_{I_1} \\ &\quad - \underbrace{1/\sqrt{2\pi P} \int_{-\infty}^0 x e^{-(x-\hat{x})^2/2P} dx}_{I_2}. \end{aligned} \quad (\text{A.1})$$

To calculate (A.1), we start with the first integral I_1 :

$$\begin{aligned} I_1 &= \frac{1}{\sqrt{2\pi P}} \int_0^{\infty} x e^{-(x-\hat{x})^2/2P} dx = \left(t = \frac{x-\hat{x}}{\sqrt{P}} \right) \\ &= \frac{1}{\sqrt{2\pi}} \int_{-\hat{x}/\sqrt{P}}^{\infty} (t\sqrt{P} + \hat{x}) e^{-t^2/2} dt \\ &= \frac{\sqrt{P}}{\sqrt{2\pi}} \int_{-\hat{x}/\sqrt{P}}^{\infty} t e^{-t^2/2} dt + \frac{\hat{x}}{\sqrt{2\pi}} \int_{-\hat{x}/\sqrt{P}}^{\infty} e^{-t^2/2} dt \\ &= \frac{\sqrt{P}}{\sqrt{2\pi}} e^{-x^2/2P} + \frac{\hat{x}}{\sqrt{2\pi}} \int_{-\hat{x}/\sqrt{P}}^{\infty} e^{-t^2/2} dt \\ &= \frac{\sqrt{P}}{\sqrt{2\pi}} e^{-x^2/2P} + \hat{x} \left(1 - \frac{1}{\sqrt{2\pi}} \int_{-\infty}^{-\hat{x}/\sqrt{P}} e^{-t^2/2} dt \right) \\ &= \frac{\sqrt{P}}{\sqrt{2\pi}} e^{-x^2/2P} + \hat{x} \left[1 - \Phi\left(\frac{-\hat{x}}{\sqrt{P}}\right) \right]. \end{aligned} \quad (\text{A.2})$$

Similar technique can be used to find the second integral I_2 :

$$\begin{aligned}
I_2 &= \frac{1}{\sqrt{2\pi P}} \int_{-\infty}^0 x e^{-(x-\hat{x})^2/2P} dx = \left(t = \frac{x-\hat{x}}{\sqrt{P}} \right) \\
&= \frac{1}{\sqrt{2\pi}} \int_{-\infty}^{-\hat{x}/\sqrt{P}} (t\sqrt{P} + \hat{x}) e^{-t^2/2} dt = \dots \\
&= -\frac{\sqrt{P}}{\sqrt{2\pi}} e^{-\hat{x}^2/2P} + \hat{x} \frac{1}{\sqrt{2\pi}} \int_{-\infty}^{-\hat{x}/\sqrt{P}} e^{-t^2/2} dt \\
&= -\frac{\sqrt{P}}{\sqrt{2\pi}} e^{-\hat{x}^2/2P} + \hat{x} \Phi\left(-\frac{\hat{x}}{\sqrt{P}}\right),
\end{aligned} \tag{A.3}$$

and finally,

$$\begin{aligned}
\hat{z} &= \mathbb{E}\left(|x| \mid y^k\right) = I_1 - I_2 = \frac{\sqrt{P}}{\sqrt{2\pi}} e^{-\hat{x}^2/2P} \\
&\quad + \hat{x} \left[1 - \Phi\left(-\frac{\hat{x}}{\sqrt{P}}\right) \right] \\
&\quad - \left[-\frac{\sqrt{P}}{\sqrt{2\pi}} e^{-\hat{x}^2/2P} + \hat{x} \Phi\left(-\frac{\hat{x}}{\sqrt{P}}\right) \right] \\
&= \sqrt{\frac{2P}{\pi}} e^{-\hat{x}^2/2P} + \hat{x} \left[1 - 2\Phi\left(-\frac{\hat{x}}{\sqrt{P}}\right) \right].
\end{aligned} \tag{A.4}$$

This completes the derivation of equation (8).

Data Availability

The data used to support the findings of this study are included within the article.

Conflicts of Interest

The authors declare that there are no conflicts of interest regarding the publication of this paper.

Acknowledgments

This study was supported by the National Research Foundation of Korea Grant funded by the Ministry of Science and ICT (NRF-2017R1A5A1015311) and the Gyeongsang National University Fund for Professors on Sabbatical Leave, 2018-2019.

References

- [1] H. B. Mitchell, *Image Fusion: Theories, Techniques and Applications*, Springer Science & Business Media, Heidelberg, Germany, 2010.
- [2] B. Ramu, "A comparison study on methods for measuring distance in images," *International Journal of Research in Computers*, vol. 1, no. 2, pp. 34–38, 2012.
- [3] L. Wang, Y. Zhang, and J. Feng, "On the Euclidean distance of images," *IEEE Transactions on Pattern Analysis and Machine Intelligence*, vol. 27, no. 8, pp. 1334–1339, 2005.
- [4] S. K. Pathi, A. Kiselev, A. Kristoffersson, D. Repsilber, and A. Loutfi, "A novel method for estimating distances from a robot to humans using egocentric RGB camera," *Sensors*, vol. 19, no. 14, pp. 3142–3155, 2019.
- [5] Y. S. Suh, N. H. Q. Phuong, and H. J. Kang, "Distance estimation using inertial sensor and vision," *International Journal of Control, Automation and Systems*, vol. 11, no. 1, pp. 211–215, 2013.
- [6] K. Murawski, "Method of measuring the distance to an object based on one shot obtained from a motionless camera with a fixed-focus lens," *ACTA Physica Polonica A*, vol. 127, no. 6, pp. 1591–1596, 2015.
- [7] F. Moreno Noguera, "3D human pose estimation from a single image via distance matrix regression," in *Proceedings of the IEEE Conference on Computer Vision and Pattern Recognition*, pp. 1561–1570, Honolulu, HI, USA, July 2017.
- [8] L. Wang, Y. Zhang, and J. Feng, "On the Euclidean distance of images," *IEEE Transactions on Pattern Analysis and Machine Intelligence*, vol. 27, no. 8, pp. 1334–1339, 2005.
- [9] M. D. Malkauthekar, "Classification of facial images," in *Proceedings of the International Conference on Emerging Trends in Electrical and Computer Technology*, pp. 507–511, Nagercoil, India, March 2011.
- [10] U. B. Gohatre and V. Patil, "Estimation of velocity and distance measurement for projectile trajectory prediction of 2D image and 3D graph in real time system," in *Proceedings of the International Conference on Energy, Communication, Data Analytics and Soft Computing (ICECDS)*, pp. 2543–2546, Chennai, India, August 2017.
- [11] J. Fabrizio and S. Dubuisson, "Motion estimation using tangent distance," in *Proceedings of the IEEE International Conference on Image Processing*, pp. 489–492, San Antonio, TX, USA, September 2007.
- [12] M. Rezaei, M. Terauchi, and R. Klette, "Robust vehicle detection and distance estimation under challenging lighting conditions," *IEEE Transactions on Intelligent Transportation Systems*, vol. 16, no. 5, pp. 2723–2743, 2015.
- [13] E. Kim and K. Kim, "Distance estimation with weighted least squares for mobile beacon-based localization in wireless sensor networks," *IEEE Signal Processing Letters*, vol. 17, no. 6, pp. 559–562, 2010.
- [14] M. Yamada, N. Kikuma, and K. Sakakibara, "Distance estimation between base station and user terminal using multi-carrier signal," in *Proceedings of the International Symposium on Antennas and Propagation*, pp. 173–174, Busan, Republic of Korea, August 2018.
- [15] P. H. Truong, S.-I. Kim, and G.-M. Jeong, "Real-time estimation of distance traveled by cart using smartphones," *IEEE Sensors Journal*, vol. 16, no. 11, pp. 4149–4150, 2016.
- [16] Y. Chen, D. Xu, H. Luo, S. Xu, and Y. Chen, "Maximum likelihood distance estimation algorithm for multi-carrier radar system," *The Journal of Engineering*, vol. 2019, no. 21, pp. 7432–7435, 2019.
- [17] B. Deng, X. Liu, and H. Wang, "Novel way of scalar miss distance measurement," in *Proceedings of the International Conference on Measuring Technology and Mechatronics Automation*, pp. 789–791, Changsha City, China, March 2010.
- [18] H. Radhika, P. T. V. Bhuvaneshwari, and P. Senthil Kumar, "An efficient distance estimation algorithm using Kalman estimator for outdoor wireless sensor network," in *Proceedings of the International Conference on Signal and Image Processing*, pp. 506–510, Changsha, China, December 2010.
- [19] X. Wang, M. Fu, and H. Zhang, "Target tracking in wireless sensor networks based on the combination of KF and MLE using distance measurements," *IEEE Trans. Mobile Computing*, vol. 11, no. 4, pp. 567–576, 2012.

- [20] L. Angrisani, A. Baccigalupi, and R. Schiano Lo Moriello, "Ultrasonic time-of-flight estimation through unscented kalman filter," *IEEE Transactions on Instrumentation and Measurement*, vol. 55, no. 4, pp. 1077–1084, 2006.
- [21] S. Theodoridis, *Machine Learning: A Bayesian and Optimization Perspective*, Academic Press, Newyork, NY, USA, 2015.
- [22] G. McLachlan, *Discriminant Analysis and Statistical Pattern Recognition*, John Wiley & Sons, Newyork, NY, USA, 2004.
- [23] J. Havelock, B. J. Oommen, and O.-C. Granmo, "Novel distance estimation methods using "stochastic learning on the line" strategies," *IEEE Access*, vol. 6, pp. 48438–48454, 2018.
- [24] H. T. Duong and Y. S. Suh, "Walking distance estimation of a walker user using a wrist-mounted IMU," in *Proceedings of the 2017 56th Annual Conference of the Society of Instrument and Control Engineers of Japan (SICE)*, pp. 1061–1064, Kanazawa, Japan, September 2017.
- [25] J. Zhang, "On the distribution of a quadratic form in normal variates," *REVSTAT Statistical Journal*, vol. 16, no. 3, pp. 315–322, 2018.
- [26] K.-H. Yuan and P. M. Bentler, "Two simple approximations to the distributions of quadratic forms," *British Journal of Mathematical and Statistical Psychology*, vol. 63, no. 2, pp. 273–291, 2010.
- [27] J. H. Clements, "Recursive maximum likelihood estimation of aircraft position using multiple range and bearing measurements," in *Proceedings of Position, Location and Navigation Symposium—PLANS '96*, pp. 199–204, Atlanta, GA, USA, April 1996.
- [28] D. E. Manolakis and A. I. Dounis, "Advances in aircraft-height estimation using distance-measuring equipment," *IEE Proceedings—Radar, Sonar and Navigation*, vol. 143, no. 1, pp. 47–52, 1996.
- [29] D. Zachariah, I. Skog, M. Jansson, and P. Händel, "Bayesian estimation with distance bounds," *IEEE Signal Processing Letters*, vol. 19, no. 12, pp. 880–883, 2012.
- [30] D. Simon, *Optimal State Estimation*, Wiley&Sons, New York, NJ, USA, 2006.
- [31] Y. Bar-Shalom, X. Li, and T. Kirubarajan, *Estimation with Applications to Tracking and Navigation*, Wiley&Sons, New York, NY, USA, 2001.